Expert Systems With Applications 259 (2025) 125356

Contents lists available at ScienceDirect

Expert Systems With Applications

journal homepage: www.elsevier.com/locate/eswa

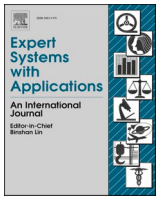

# A novel grey seasonal model with time power for energy prediction

Weijie Zhou [a,b,d], Jiaxin Chang [a,b], Huimin Jiang [a,b], Song Ding [c,e,*], Rongrong Jiang [a,b], Xupeng Guo [f]

[a] School of Wu Jinglian Economics, Changzhou University, Changzhou 213159, China
[b] School of Business, Changzhou University, Changzhou 213159, China
[c] School of Economics, Zhejiang University of Finance and Economics, Hangzhou 310018, China
[d] Jiangsu Energy Strategy Research Base, Changzhou University, Changzhou 213159, China
[e] Zhejiang Institute of "Eight-Eight" Strategies, Hangzhou 310018, China
[f] Office of the Leading Group for Digital Reform, Hangzhou Normal University, Hangzhou 311121, China

ARTICLE INFO

*Keywords:*
Grey prediction model
Seasonal time series
Time power item
Cultural algorithm
Energy prediction

ABSTRACT

The fluctuation of seasonal time series has attracted considerable attention. However, the complexity of socio-economic development and the variability of influencing factors make accurate predictions of seasonal time series more difficult. A new discrete grey seasonal model, namely *DGSTPM(1,1)*, is established, which employs the time power term based on the cultural algorithm to effectively deal with the time sequences characterized by nonlinear tendency and periodic fluctuations. Firstly, the operating mechanism of the *DGSTPM(1,1)* model is expounded by combining the time power item with the traditional grey seasonal model to enhance the forecasting capability. Then, the optimal time power index of the model can be determined by incorporating the cultural algorithm. Subsequently, several properties are thoroughly discussed to illustrate the superiority and uniformity of the new model. Finally, two energy-related cases with different data features and sample sizes are applied to identify the efficacy and robustness of the *DGSTPM(1,1)* model, referring to monthly crude oil production in the United States and quarterly coke production in China. Based on the various error criteria, SPA and DM tests, the results indicate that the *DGSTPM(1,1)* outperforms its competitors both in simulation and prediction phases, including *DGSTM(1,1), SGM(1,1), SDTGM, FTGM, SARIMA, LSSVM, BPNN,* and *LSTM* models. Meanwhile, the new model can effectively address seasonal time series with nonlinear characteristics owing to its dynamic time power item with the support of the cultural algorithm.

## 1. Introduction

A precise forecast can give a theoretical foundation for establishing sound strategies for future social and economic growth (Li, Li, Ding, Cao, & Li, 2023; Ding & Zhang, 2023). In reality, time series often exhibit volatility and seasonality due to various influences and random occurrences. Given seasonal data's cyclical regularity and trend volatility, effective prediction has remained a significant research challenge. To address seasonal series features, research approaches primarily include statistical models, machine learning techniques, neural network models, grey prediction methods, and hybrid models integrating grey forecasting with other methodologies. These approaches aim to better characterize series with seasonal characteristics. Table 1 provides an overview of the latest representative seasonal forecasting methods.

As a traditional forecasting method, statistical models eliminate seasonal components from time series data in order to generate a relatively stable series and thereby achieve the objective of accurate prediction. To account for seasonal fluctuations in the weather, Gupta & Christopher (2009) developed a multivariate statistical model to evaluate PM2.5 concentration at 85 monitoring locations in the southeastern United States. Furthermore, by researching the seasonal features of infection, Mao, Zhang, & Yan (2018) used *SARIMA* to estimate the occurrence of tuberculosis in China and established practical and reliable preventative programs. To properly anticipate heat demand, Fang & Lahdelma (2016) employed *SARIMA* with a linear regression model.

In the last two years, the coronavirus has multiplied at an alarming rate. Accurate coronavirus prediction can aid the medical and healthcare systems in developing sensible plans to combat the pandemic.

* Corresponding author.
*E-mail addresses:* wjzhou@cczu.edu.cn (W. Zhou), 276397688@qq.com (J. Chang), s21081202002@smail.cczu.edu.cn (H. Jiang), dingsong1129@163.com (S. Ding), 2601168956@qq.com (R. Jiang), guo@hznu.edu.cn (X. Guo).

https://doi.org/10.1016/j.eswa.2024.125356
Received 1 October 2022; Received in revised form 15 February 2024; Accepted 6 September 2024
Available online 10 September 2024

**Table 1**
Representative forecasting technique for seasonal predictions.

| Category | Authors | Model description | Frequency | Case |
|---|---|---|---|---|
| Statistical models | Gupta & Christopher (2009) | Multiple regression methods | Hourly | PM2.5 concentrations at 85 monitoring sites in the southeastern United States |
| | Valipour (2015) | *SARIMA*+*ARIMA* | Annually | Long-term runoff forecasting in the United States |
| Artificial intelligences | Chen, Yang, & Liu (2015) | *ESPLSSVM* (Empirical mode decomposition with PSO and *LSSVM*) | weekly | The electric load data of South Australia (SA) from 1999 to 2012 |
| | Li, Liang, & Lu (2020) | K-means algorithm with (*PSO-LSSVM*) algorithm | Daily | The daily tourist data for Mountain Huangshan during the period between 2014 and 2017 |
| Grey (hybrid) prediction models | Wang, Li, & Pei (2018) | A seasonal grey model | Quarterly | The primary industries in China from 2010 to 2016 |
| | Carmona-Benítez & Nieto (2020) | *SARIMA* Damp Trend Grey Forecasting Model | Quarterly | The United States domestic air transport market between 1993 and 2017 |

ArunKumar, Kalaga, & Kumar (2021) employed *ARIMA* and *SARIMA* to predict the dynamics of the cumulative COVID-19 cases in the top 16 nations, and the findings revealed that the *SARIMA* model had a better prediction impact. Valipour (2015) has used *SARIMA* and *ARIMA* to predict long-term runoff in the United States, demonstrating that *SARIMA* had a more substantial prediction impact on such seasonal series. Furthermore, many researchers utilized *SARIMA* to forecast seasonal series of airport passenger flow (Tsui, Balli, & Gilbey, 2014), inflation (Saz, 2011), and sugarcane output (Mwanga, Ong'ala, & Orwa, 2017). While these statistical models often exhibit a reasonable prediction trend, they are susceptible to random occurrences and may struggle to capture the nonlinear properties inherent in sequences (Ding, 2019; Wei, Xie, & Yang, 2020). Moreover, verifying the accuracy of forecasts typically requires large samples, and addressing the prediction effectiveness of short-term series and volatility remains a challenge (Tang, Yu, & He, 2014). To overcome these limitations, researchers have explored alternative approaches such as machine learning techniques and hybrid models that integrate multiple forecasting methodologies.

Machine learning techniques based on big data have the adaptive potential to capture sequence fluctuation signals more sensitively and better deal with nonlinear features in seasonal time series. Kaytez (2020) proposed a hybrid model based on the *LSSVM* model to enhance the prediction accuracy of Turkey's electricity consumption. Martínez, Frías, & Pérez-Godoy (2018) employed *KNN* regression to handle seasonal information in order to improve prediction accuracy. At daily and monthly scales, Nourani & Behfar (2021) effectively utilized seasonal *LSTM* for runoff and sediment prediction. Machine learning methods combine the advantages of various approaches to produce a series of combined forecasts, which are also extensively employed in seasonal series, to increase prediction accuracy. Lu, Zhang, & Chen (2021) coupled the *ARIMA* model and the *LSTM* neural network to estimate short-term real-time traffic flow. Chen, Yang, & Liu (2015) constructed a power load prediction model based on *LSSVM* and the particle swarm optimization technique, and tested it using power data from southern Australia. Farajzadeh & Alizadeh (2018) suggested a hybrid model (*W-S-LSSVM*) that included the discrete wavelet transform, *ARIMAX*, and *LSSVM* to increase rainfall time series prediction accuracy. To accurately estimate the daily flow of tourists in Huangshan Scenic Spot, Li, Liang, & Lu (2020) employed the k-means algorithm, and the particle swarm optimization-least squares support vector Machine (*PSO-LSSVM*) technique. In addition, to address the regulatory safety issues of hydropower *DAMS*, a model that hybridizes the multiple regression, *SARIMA*, and backpropagation neural network (*BPNN*) was devised, and its effectiveness was verified by using dam data from Vietnam (Zou, Bui, & Xiao, 2018). Khwaja, Anpalagan, & Naeem (2020) trained the neural network by combining the two methods of bagging and pressurization to reduce the fluctuation error of data and constructed an integrated machine learning method based on the artificial neural network to improve short-term power load. The results indicated that the combined prediction method outperforms other single models. Although the artificial neural network model can deal with the nonlinear characteristics of seasonal series, it cannot directly reflect the relationship between variables because it needs to control a range of parameters and is constrained by the objective constraints of insufficient data (Chen, Chang, & Zhuang, 2020; Xiao, & Duan, 2020).

To accomplish the effect of precise modeling, the above machine learning and statistical models frequently demand a large amount of data. In fact, the sequence typically has the features of incomplete information due to the rapid emergence of some new objects and diverse statistical calibers. Faced with such a complicated and information-poor system, Professor Deng established the grey system theory and built a grey prediction model to investigate the system's rules. Although the traditional grey models have many advantages as small sample size and high prediction accuracy, which use widely in energy (Yuan, Liu, & Fang, 2016), pollutants (Wang, Cai, & Xu, 2014), passenger flow (Liu, Peng, & Bai, 2014), and other fields (Zhou & He, 2013; Chen & Huang, 2013), they cannot accurately describe the seasonality of the sequence.

As a result, to widen the application span of the grey model, several academics have come up with novel ways. Wang, Li, & Pei (2018) constructed the *SGM(1,1)* model that can improve the flexibility of the traditional grey models to seasonal sequences and the model has been successfully applied to forecast Turkey's monthly electricity demand from 2015 to 2020. Wang, Wang, & Li (2020) incorporated dynamic adjustment factors into the grey seasonal model to improve the model's accuracy. Zhou, Wu, & Ding (2020) constructed a seasonal nonlinear grey Bernoulli model to better predict air quality indicators in the Yangtze River Delta region in order to comprehend the nonlinear and seasonal aspects of the series. Ye, Xie, John E, & Shang (2024) proposed the Fourier Time-Varying Grey Model (*FTGM*) to improve seasonal demand forecasting accuracy in supply chain management, overcoming challenges of changing trends and limited data, with experimental results showcasing its superiority over traditional methods for retail companies. Carmona-Benítez & Nieto (2020) utilized a dynamic seasonal damping factor to enhance the Damped Trend Grey Model (*DTGM*) and proposed the Seasonal Autoregressive Integrated Moving Average Damped Trend Grey Forecasting Model (*SDTGM*) for predicting passenger demand within the aviation industry's route network. Based on the novel information-first cycle accumulation operator, Zhou, Tao, Chang, Jiang, & Chen (2023) proposed the *NCGHW* model. They utilized the *LBFGS* algorithm to find the most suitable parameters for this model, aiming to efficiently predict the total power consumption in China.

Furthermore, Li, Liu, & Lv (2021) proposed the grey seasonal model with cumulative new information priority to accurately forecast China's housing prices, demonstrating its efficacy. Given the seasonality of short-time traffic, Xiao, Yang, & Mao (2017) developed a modified rolling grey seasonal prediction model that leverages the cyclic truncation cumulative generation operation to eliminate random sequence disturbance, resulting in a model with high adaptability. Chen, Pei, & Zhao (2021) used the buffer operator in conjunction with *DGGM(1,1)* to appropriately predict power data seasonal fluctuations. Zhou & Ding (2021) constructed the *DGSM(1,1)* model combined with dummy variables. A representative case was applied to verify the validation of the

*DGSM(1,1) model*, providing a reference for the prediction of seasonal fluctuation series. Li & Qi (2024) proposed the Fourier modified grey forecasting model (*FDSGM(1, 1, x(β),γ)*) based on the seasonal fluctuation characteristics and initial condition optimization. To better capture the trend changes of time series, Zhou et al. (2021) introduced the time trend term to the *DGSM(1,1)* and established *DGSTM(1,1)* model for further improving the prediction accuracy.

Under specific conditions, a suite of intelligent optimization algorithms, inspired by human intelligence and social or natural phenomena of biological groupings can enhance model accuracy through parameter optimization (Ding, Hu, & Lin, 2023). Consequently, to broaden the scope of application and enhance the stability of the model, several researchers have integrated intelligent algorithms with grey prediction models. Considering both seasonal and periodic variations in monthly natural gas production, Li, Wang, & Wu (2021) proposed a fractional cumulative non-uniform discrete grey season model (*PFSM(1,1)*) that incorporates particle swarm optimization to enhance the predictive capability of the model for seasonal series. The hybrid optimization grey seasonal change index model proposed by Xiong, Hu, & Guo (2021) was enhanced by integrating the whale optimization algorithm, resulting in a significant improvement in prediction accuracy and speed for residential electricity consumption. In order to predict the settling of a high-speed soft soil foundation, Qian & Dang (2012) introduced the power of time into the classic grey model. Liu, Xie, & Lao (2020) create an innovative grey prediction model with time power by integrating the linear interpolation approach and quantum genetic algorithm, enabling accurate estimation of China's GDP. Ding, Li, & Wu (2021) proposed an adaptive grey model with adjustable time power to enhance forecasting performance. They substantiated the superiority of this model by utilizing nuclear energy data from China and the United States.

Although *DGSTM(1,1)* has previously demonstrated high prediction accuracy, its time trend term is linear, making in unsuitable for seasonal sequences with nonlinear characteristics. In this paper, a time power item that can capture nonlinear feature of seasonal time series is introduced to *DGSTM(1,1)* model, and the new *DGSTPM(1,1)* model is established. Meanwhile, considering the superiority of intelligent optimization algorithms in grey prediction models, the culture algorithm is employed to optimize the power index. The novel model is then utilized to simulate and predict oil consumption and coke production, thereby validating its efficacy.

Compared with previous grey prediction models on seasonal series, the new model mainly has the following innovations:

(1) The new model, incorporating the power time term, not only effectively handles the periodicity and fluctuation characteristics of diverse seasonal time series but also demonstrates applicability to nonlinear features in seasonal sequences, thereby expanding its application scope and enhancing prediction capability.
(2) By utilizing the cultural algorithm, the optimal hyper-parameter, namely the time power index, can be effectively determined to ensure that the model exhibits high stability and adaptability. Experimental results demonstrate that this algorithm significantly enhances prediction performance.
(3) This paper selects two energy-related seasonal time series, each characterized by distinct fluctuations and sample lengths. Additionally, to verify the universality and stability of the new model, eight competing models along with two rarely utilized statistical tests (i.e., SPA and DM) are employed.

The remaining part of this research is organized as follows. Section 2 provides a comprehensive discussion on the mechanism and properties of the novel model. Subsequently, in section 3, we demonstrate the effectiveness and robustness of the novel model by utilizing two cases with different characteristics and sample sizes. Lastly, Section 4 presents a concise summary of the main conclusions.

## 2. Methods and properties

We propose a discrete grey seasonal model, denoted as *DGSTPM (1,1)*, in this paper. Moreover, the cultural algorithm is employed to determine the time power index of the *DGSTPM(1,1)* model and address the limitations of the conventional *DGSTM (1,1)* model. Additionally, we discuss various properties of *DGSTPM(1,1)*.

### 2.1. Mechanism of the proposed model

In the *DGSTM(1,1)* model, the time term can be utilized to depict the trend in the series; however, due to its linearity, it fails to capture the nonlinear fluctuations present in seasonal data. Henceforth, we introduce a time power term to remedy this limitation within the *DGSTM (1,1)* model. Specifically, this time power term $\xi t^{\gamma}$ replaces the conventional linear time term $\beta t$. In addition, the optimal time power index $\gamma$ of the *DGSTPM(1,1)* model can be determined by employing the Culture Algorithm and some error criteria. Furthermore, it is noteworthy that both *DGSTM(1,1)* and *DGSM(1,1)* models are regarded as special cases of *DGSTPM(1, 1)* (see section 2.3), thereby indicating that our proposed model possesses greater generality. The modeling process for this new model is displayed as follows.

**Definition 1.** *Initially,* $\boldsymbol{S}^{(\mathbf{0})} = \left(s^{(0)}(1), s^{(0)}(2), \cdots, s^{(0)}(n)\right)$ *is defined as a non-negative seasonal time series. Additionally, the period of* $\boldsymbol{S}^{(\mathbf{0})}$ *is denoted by the c. The cumulative sequence* $\boldsymbol{S}^{(\mathbf{1})} = \left(s^{(1)}(1), s^{(1)}(2), \cdots, s^{(1)}(n)\right)$ *is obtained by accumulating the original sequence* $\boldsymbol{S}^{(\mathbf{0})}$*, where* $s^{(1)}(t) = \sum_{i=1}^{t} s^{(0)}(i)$*,* $t = 1, 2, \cdots, n$*. To mitigate irregularity and random noise in the original sequence, preprocessing of raw data is conducted, i.e., the accumulating operation for the he original sequence* $\boldsymbol{S}^{(\mathbf{0})}$ *and we obtain the sequence* $\boldsymbol{S}^{(\mathbf{1})}$.

**Definition 2.** *The proposed discrete grey seasonal model (one variable and first-order) is defined as .*

$$s^{(1)}(t+1) = \eta s^{(1)}(t) + \xi t^{\gamma} + \sigma_{M(t+1,c)} \tag{1}$$

*where* $\xi t^{\gamma}$ *and* $\sigma_{M(t+1,c)}$ *represent the time power term and seasonal factor, respectively.* $\gamma$ *is the time power index, which is determined by using the cultural algorithm. And the* $M(t,c)$ *is defined as*

$$M(t,c) = \begin{cases} c & \text{t mod c} = 0 \\ \text{t mod c} & \text{t mod c} \neq 0 \end{cases} \tag{2}$$

*Furthermore, we assume that the parameters* $\xi$*,* $\gamma$ *and* $\sigma_{M(t+1,c)}$ *have been estimated. The new model can be better illustrated by an example of quarterly data (c = 4) with two full cycles (n = 8 and t = 1, 2..., 8), i.e.,*

$$\begin{aligned}
s^{(1)}(2) &= \widehat{\eta} s^{(1)}(1) + \widehat{\xi} * 1^{\widehat{\gamma}} + \widehat{\sigma}_2 \\
s^{(1)}(3) &= \widehat{\eta} s^{(1)}(2) + \widehat{\xi} * 2^{\widehat{\gamma}} + \widehat{\sigma}_3 \\
s^{(1)}(4) &= \widehat{\eta} s^{(1)}(3) + \widehat{\xi} * 3^{\widehat{\gamma}} + \widehat{\sigma}_4 \\
s^{(1)}(5) &= \widehat{\eta} s^{(1)}(4) + \widehat{\xi} * 4^{\widehat{\gamma}} + \widehat{\sigma}_1 \\
s^{(1)}(6) &= \widehat{\eta} s^{(1)}(5) + \widehat{\xi} * 5^{\widehat{\gamma}} + \widehat{\sigma}_2 \\
s^{(1)}(7) &= \widehat{\eta} s^{(1)}(6) + \widehat{\xi} * 6^{\widehat{\gamma}} + \widehat{\sigma}_3 \\
s^{(1)}(8) &= \widehat{\eta} s^{(1)}(7) + \widehat{\xi} * 7^{\widehat{\gamma}} + \widehat{\sigma}_4
\end{aligned} \tag{3}$$

*If the time power index* $\gamma$ *is set, we will have the parameters of the quarterly data by applying the OLS technique,* $\widehat{\boldsymbol{P}} = (\widehat{\eta}, \widehat{\xi}, \widehat{\sigma}_1, \widehat{\sigma}_2, \widehat{\sigma}_3, \widehat{\sigma}_4)^T$*, where the* $\widehat{\xi}$ *is the coefficient of time power term. We can also get the parameters of monthly data(c = 12),* $\widehat{\boldsymbol{P}} = (\widehat{\eta}, \widehat{\xi}, \widehat{\sigma}_1, \widehat{\sigma}_2, \cdots, \widehat{\sigma}_{12})^T$*. For a generalized parameter estimation,* $\widehat{\boldsymbol{P}} = (\widehat{\eta}, \widehat{\xi}, \widehat{\sigma}_1, \widehat{\sigma}_2, \cdots, \widehat{\sigma}_c)^T$ *will be denoted in* Theorem 1.

**Theorem 1.** *The formula* $\widehat{P} = (\widehat{\eta}, \widehat{\xi}, \widehat{\sigma}_1, \widehat{\sigma}_2, \cdots, \widehat{\sigma}_c)^T$ *is explicated in Definition 2, and its values can be obtained through the utilization of Ordinary Least Squares (OLS), denoted as* $\widehat{\mathbf{P}} = \left(\mathbf{B}^{\mathbf{T}}\mathbf{B}\right)^{-1}\mathbf{B}^{\mathbf{T}}\mathbf{Y}$*, wherein the parameters* $\boldsymbol{B}$ *and* $\boldsymbol{Y}$ *are designated as,*

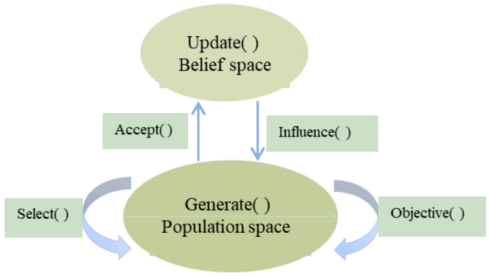


**Begin**
Set p=0
Initialize generate population POP (p);
Initialize Belif space BLF (p);
Evaluate Population POP (p);
**Repeat**
Communicate (POP (P),BLF (p));
Adjust BLF (p);
Keep communicating (POP (p),BLF (p));
p=p+1;
Selecting (POP(p)) from p-1;
**Until** (termination condition)
**End**

**Fig. 1.** The basic framework and pseudo-code of the cultural algorithms.

$$\boldsymbol{B}=\begin{bmatrix} s^{(1)}(1) & 1 & 0 & 1 & 0 & \cdots & \cdots & \cdots & 0 \\ s^{(1)}(2) & 2^{\gamma} & 0 & 0 & 1 & \cdots & \cdots & \cdots & 0 \\ \vdots & \vdots & \vdots & \vdots & \vdots & \vdots & \vdots & \vdots & \vdots \\ s^{(1)}(c-1) & (c-1)^{\gamma} & 0 & 0 & 0 & \cdots & \cdots & \cdots & 1 \\ s^{(1)}(c) & c^{\gamma} & 1 & 0 & 0 & \vdots & \vdots & \vdots & 0 \\ \vdots & \vdots & \vdots & \vdots & \vdots & \vdots & \vdots & \vdots & \vdots \\ s^{(1)}(n-1) & (n-1)^{\gamma} & \cdots & \cdots & \cdots & \cdots & 1 & \cdots & 0 \end{bmatrix}, Y = \begin{bmatrix} s^{(1)}(2) \\ s^{(1)}(3) \\ \vdots \\ s^{(1)}(n) \end{bmatrix} \tag{4}$$

**Proof.** Substituting $s^{(1)}(t)$ into Eq. (1), we will obtain

$$\begin{cases} s^{(1)}(2)=\widehat{\eta}s^{(1)}(1)+\widehat{\xi}_1\cdot 1+0\cdot\widehat{\sigma}_1+1\cdot\widehat{\sigma}_2+0\cdot\widehat{\sigma}_3+\cdots+0\cdot\widehat{\sigma}_c \\ s^{(1)}(3)=\widehat{\eta}s^{(1)}(2)+\widehat{\xi}_1\cdot 2^{\gamma}+0\cdot\widehat{\sigma}_1+0\cdot\widehat{\sigma}_2+1\cdot\widehat{\sigma}_3+\cdots+0\cdot\widehat{\sigma}_c \\ \vdots \\ s^{(1)}(c)=\widehat{\eta}s^{(1)}(c-1)+\widehat{\xi}_1\cdot(c-1)^{\gamma}+0\cdot\widehat{\sigma}_1+0\cdot\widehat{\sigma}_2+0\cdot\widehat{\sigma}_3+\cdots+1\cdot\widehat{\sigma}_c \\ s^{(1)}(c+1)=\widehat{\eta}s^{(1)}(c)+\widehat{\xi}_1\cdot c^{\gamma}+1\cdot\widehat{\sigma}_1+0\cdot\widehat{\sigma}_2+0\cdot\widehat{\sigma}_3+\cdots+0\cdot\widehat{\sigma}_c \\ \vdots \\ s^{(1)}(n)=\widehat{\eta}s^{(1)}(n-1)+\widehat{\xi}_1\cdot(n-1)^{\gamma}+\cdots+1\cdot\widehat{\sigma}_{M(n,c)}+\cdots+0\cdot\widehat{\sigma}_c \end{cases} \tag{5}$$

Then, Eq. (5) can be converted to a matrix $\mathbf{Y}=\mathbf{B}\widehat{\mathbf{P}}$. By utilizing the *OLS* method, the parameter can be obtained as $\widehat{\mathbf{P}}=\left(\mathbf{B}^{\mathrm{T}}\mathbf{B}\right)^{-1}\mathbf{B}^{\mathrm{T}}\mathbf{Y}$.

**Theorem 2.** *Supposing that* $\widehat{\boldsymbol{P}}=(\widehat{\eta},\widehat{\xi},\widehat{\sigma}_1,\widehat{\sigma}_2,\cdots,\widehat{\sigma}_c)^T$ *and* $\gamma$ *are known, the time response for generating simulations and forecasts of the proposed model DGSTPM(1,1)is described below:*

$$\widehat{s}^{(1)}(t)=\widehat{\eta}^{t-1}s^{(0)}(1)+\sum_{a=1}^{t-1}\widehat{\eta}^{t-1-a}a^{\gamma}\widehat{\xi}+\sum_{a=2}^{t}\widehat{\eta}^{t-a}\widehat{\sigma}_{M(a,c)},t\geqslant 2 \tag{6}$$

The corresponding predictive function is generated by employing the 1-IAGO:

$$\begin{aligned}\widehat{s}^{(0)}(t)&=\widehat{\eta}^{t-2}(\widehat{\eta}-1)s^{(0)}(1)+\sum_{a=2}^{t-1}\widehat{\eta}^{t-1-a}(a^{\gamma}-(a-1)^{\gamma})\widehat{\xi} \\ &+\widehat{\eta}^{t-2}\widehat{\xi}+\widehat{\eta}^{t-2}\widehat{\sigma}_2+\sum_{a=3}^{t}\widehat{\eta}^{t-a}\left(\widehat{\sigma}_{M(a,c)}-\widehat{\sigma}_{M(a-1,c)}\right),t\geqslant 2\end{aligned} \tag{7}$$

where $\widehat{s}^{(1)}(1)=\widehat{s}^{(0)}(1)=s^{(0)}(1)$, If $m_2<m_1,\sum_{a=m_1}^{m_2}\widehat{\eta}^{t-a}\sigma_{M(a,c)}=0$, then

$$\widehat{s}^{(1)}(t+1)=\widehat{\eta}^{t}s^{(0)}(1)+\sum_{a=1}^{t}\widehat{\eta}^{t-a}a^{\gamma}\widehat{\xi}+\widehat{\eta}^{t-1}\widehat{\sigma}_2+\sum_{a=3}^{t+1}\widehat{\eta}^{t+1-a}\widehat{\sigma}_{M(a,c)}$$

**Proof.** Theorem 2 will be demonstrated through the utilization of mathematical modeling mechanism.

When $t=2$, through Eq. (1), it will obtain

$$\widehat{s}^{(1)}(2)=\widehat{\eta}\widehat{s}^{(1)}(1)+\widehat{\xi}+\widehat{\sigma}_2=\widehat{\eta}^{2-1}\widehat{s}^{(0)}(1)+\widehat{\eta}^{2-1-1}1^{\gamma}\widehat{\xi}+\widehat{\sigma}_2 \tag{8}$$

Supposing Eq.(6) is correct when $t=b$, we will verify whether Eq.(6) is satisfied when $t=b+1$.

$$\begin{aligned}\widehat{s}^{(1)}(b+1)&=\widehat{\eta}s^{(1)}(b)+b^{\gamma}\widehat{\xi}+\widehat{\sigma}_{M(b+1,c)} \\ &=\widehat{\eta}\left(\widehat{\eta}^{b-1}s^{(0)}(1)+\sum_{a=1}^{b-1}\widehat{\eta}^{b-1-a}a^{\gamma}\widehat{\xi}+\widehat{\eta}^{b-2}\widehat{\sigma}_2+\sum_{a=3}^{b}\widehat{\eta}^{b-a}\widehat{\sigma}_{M(a,c)}\right) \\ &+b^{\gamma}\widehat{\xi}+\widehat{\sigma}_{M(b+1,c)} \\ &=\widehat{\eta}^{b}s^{(0)}(1)+\sum_{a=1}^{b-1}\widehat{\eta}^{b-a}a^{\gamma}\widehat{\xi}+\widehat{\eta}^{b+1-2}\widehat{\sigma}_2+\sum_{a=3}^{b}\widehat{\eta}^{b+1-a}\widehat{\sigma}_{M(a,c)}+\widehat{\eta}^{b-b}b^{\gamma}\widehat{\xi} \\ &+\widehat{\eta}^{b+1-(b+1)}\widehat{\sigma}_{M(b+1,c)} \\ &=\widehat{\eta}^{b}s^{(0)}(1)+\sum_{a=1}^{b}\widehat{\eta}^{b-a}a^{\gamma}\widehat{\xi}+\widehat{\eta}^{b+1-2}\widehat{\sigma}_2+\sum_{a=3}^{b+1}\widehat{\eta}^{b+1-a}\widehat{\sigma}_{M(a,c)}\end{aligned} \tag{9}$$

According to Eq. (8) and Eq. (9), it can be inferred that the expression of the time response in the new model is accurate. Subsequently, we employ the inverse first-order cumulative generation operator (*1-IAGO*) to derive the predictive function in its original domain.

$$\begin{aligned}&\widehat{s}^{(0)}(t)=\widehat{s}^{(1)}(t)-\widehat{s}^{(1)}(t-1) \\ &=\widehat{\eta}^{t-1}s^{(0)}(1)+\sum_{a=1}^{t-1}\widehat{\eta}^{t-1-a}a^{\gamma}\widehat{\xi}+\widehat{\eta}^{t-2}\widehat{\sigma}_2+\sum_{a=3}^{t}\widehat{\eta}^{t-a}\widehat{\sigma}_{M(a,c)} \\ &-\left[\widehat{\eta}^{t-2}s^{(0)}(1)+\sum_{a=1}^{t-2}\widehat{\eta}^{t-2-a}a^{\gamma}\widehat{\xi}+\widehat{\eta}^{t-3}\widehat{\sigma}_2+\sum_{a=3}^{t-1}\widehat{\eta}^{t-1-a}\widehat{\sigma}_{M(a,c)}\right] \\ &=\widehat{\eta}^{t-2}(\widehat{\eta}-1)s^{(0)}(1)+\sum_{a=2}^{t-1}\widehat{\eta}^{t-1-a}(a^{\gamma}-(a-1)^{\gamma})\widehat{\xi}+\widehat{\eta}^{t-2}\widehat{\xi}+\widehat{\eta}^{t-2}\widehat{\sigma}_2 \\ &+\widehat{\eta}^{t-3}(\widehat{\sigma}_3-\widehat{\sigma}_2)\qquad\qquad+\sum_{a=4}^{t}\widehat{\eta}^{t-a}\left(\widehat{\sigma}_{M(a,c)}-\widehat{\sigma}_{M(a-1,c)}\right) \\ &=\widehat{\eta}^{t-2}(\widehat{\eta}-1)s^{(0)}(1)+\sum_{a=2}^{t-1}\widehat{\eta}^{t-1-a}(a^{\gamma}-(a-1)^{\gamma})\widehat{\xi}+\widehat{\eta}^{t-2}\widehat{\xi} \\ &+\widehat{\eta}^{t-2}\widehat{\sigma}_2\qquad\qquad+\sum_{a=3}^{t}\widehat{\eta}^{t-a}\left(\widehat{\sigma}_{M(a,c)}-\widehat{\sigma}_{M(a-1,c)}\right)\end{aligned} \tag{10}$$

At this point, the expression for $\widehat{s}^{(0)}(t)$ is proved by Eq.(10). In summary, the newly developed model's simulated and forecasted values for the seasonal series can be obtained based on the aforementioned two theorems.

### 2.2. Parameter optimization of time power index

This section primarily delineates the parameter optimization process

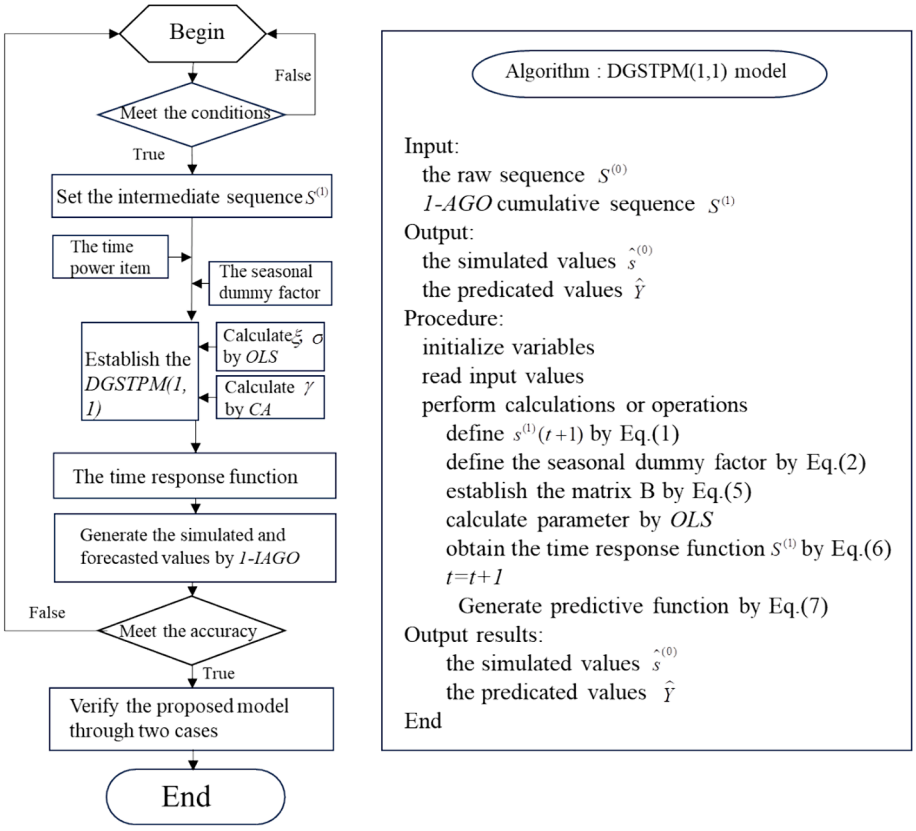


**Fig. 2.** The flow chart and pseudo-code of the *DGSTPM(1,1)* model.

for the time power index $\gamma$ within the *DGSTPM(1,1)* model, where the optimal parameters are determined through the application of the Cultural Algorithm (*CA*). Reynolds (1994) first put forward the *CA* technique to guide the search process based on the principle of human social evolution. To provide a more intuitive understanding of the operation process of the Cultural Algorithm, Fig. 1 illustrates its fundamental framework and presents its pseudo-code. The Cultural Algorithm technique primarily consists of three core components: the population space, belief space, and communication protocol. It serves as a knowledge-based evolutionary model that incorporates both population and belief spaces. The evolution of these two spaces occurs concurrently and is linked through a set of communication protocols composed of the influence () and Accept () functions.

To elaborate further, the Accept() function transmits individual experiences gained during the spatial evolution of the population to the belief space. In the belief space, these experiences are optimized and selected according to specific rules, utilizing the Update() function for spatial updates. On the other hand, the Influence() function guides the optimization of the population space by leveraging the empirical knowledge stored in the belief space, thereby enhancing the evolutionary efficiency of the population space. The Fitness() function is responsible for evaluating the fitness of individuals within the population space. Meanwhile, the Generate() function generates the next generation based on specific conditions and rules. Finally, the Select() function is tasked with selecting excellent individuals from the newly produced individuals to serve as the parents of the next generation individuals. The two-layer evolutionary mechanism, as described by the functions Accept(), Update(), Influence(), Fitness(), Generate(), and Select(), facilitates the optimization of the *DGSTPM(1,1)* model. By iteratively and repetitively applying the five functions above until a predetermined condition is met, we actively contribute to determining the optimal parameter, i.e., the time power index $\gamma$ for *DGSTPM(1,1),* and improving data adaptability. In this paper, we select the error minimization principles, seen in Eqs. (11) and (12), to search for the optimal parameter in the *DGSTPM(1,1)* model. Fig. 2 illustrates the optimization process of the time power index $\gamma$ using the *CA* algorithm within the *DGSTPM(1,1)* model and the estimation procedure for other parameters. Additionally, it provides the pseudo-code for modeling the *DGSTPM(1,1)* model.

$$\underset{\gamma}{\text{argmin}} MAPE = \frac{1}{n}\sum_{i=1}^{n}\left|\frac{\left(\hat{x}^{(0)}(t)-x^{(0)}(t)\right)}{x^{(0)}(t)}\right| \times 100\% \tag{11}$$

$$s.t.\begin{cases} \widehat{P} = (\widehat{\eta}, \widehat{\xi}, \widehat{\sigma}_1, \widehat{\sigma}_2, \cdots, \widehat{\sigma}_c)^T = \left(\mathbf{B}^{\mathrm{T}}\mathbf{B}\right)^{-1}\mathbf{B}^{\mathrm{T}}\mathbf{Y} \\ \widehat{s}^{(1)}(t) = \widehat{\eta}^{t-1}s^{(0)}(1) + \sum_{a=1}^{t-1}\widehat{\eta}^{t-1-a}a^{\gamma}\widehat{\xi} + \sum_{a=2}^{t}\widehat{\eta}^{t-a}\widehat{\sigma}_{M(a,c)} \\ \widehat{s}^{(0)}(t) = \widehat{s}^{(1)}(t) - \widehat{s}^{(1)}(t-1) \end{cases} \tag{12}$$

### 2.3. Properties of the proposed model

The new model, based on the traditional seasonal grey model composed of *DGSTM(1,1)* and *DGM(1,1)*, incorporates a time power term to enhance its applicability and robustness for time series exhibiting nonlinear tendencies and periodic fluctuation characteristics. In this part, we will provide detailed explanations and mathematical derivation regarding the properties of the established model.

**Property 1**. *The established model can integrate multiple traditional grey models.*

(1) *When* $\gamma = 1$, *the DGSTPM(1,1) model degenerates into a classical DGSTM(1,1) model.*
(2) *When* $\xi = 0$, *the DGSTPM(1,1) model becomes the DGSM(1,1) model.*

**Table 2**
Accuracy grade of MAPE.

| MAPE | ≤10 % | 10 %-20 % | 20 %-50 % | ≥50 % |
|---|---|---|---|---|
| Evaluation | Highly accurate | Good | Reasonable | Inaccurate |

**Proof:** When $\gamma = 1$, it means that the time power index is eliminated from Eq. (1), and the *DGSTPM(1,1)* is transformed into the *DGSTM(1,1)* model. Moreover, when $\xi = 0$, the original time series don't have the time term, and *DGSTPM(1,1)* is converted to the *DGSM(1,1)* model.

According to property 1, we can find that the new model can be extended from other grey discrete models. It effectively incorporates temporal dynamics and seasonal factors to address the trend characteristics of seasonal sequences, thereby enhancing model performance.

**Property 2.** *The new model exhibits unbiased and stability throughout the fitting process. Expressly, we assume that the time series* $\widehat{\boldsymbol{S}}^{(\mathbf{0})} = (\widehat{s}^{(0)}(1), \widehat{s}^{(0)}(2), \cdots, \widehat{s}^{(0)}(n))$ *is simulated based on the original series* $\boldsymbol{S}^{(\mathbf{0})}$. *In the same way, the new sequence* $\widehat{\widehat{\boldsymbol{S}}}^{(\mathbf{0})} = \left(\widehat{\widehat{s}}^{(0)}(1), \widehat{\widehat{s}}^{(0)}(2), \cdots, \widehat{\widehat{s}}^{(0)}(n)\right)$ *is simulated by utilizing DGSTPM(1,1) model for series* $\widehat{\boldsymbol{S}}^{(\mathbf{0})}$. *Then, we can get* $\widehat{\widehat{s}}^{(0)}(t) = \widehat{s}^{(0)}(t), t = 1, 2, \cdots, n$.

***Proof:*** *We verify the property 2 by taking the inverse procedure of Theorem 2. By using the proposed model, the corresponding simulation values* $\widehat{s}^{(0)}(t)$ *of the original sequence* $\boldsymbol{S}^{(\mathbf{0})}$ *can be obtained:*

**Table 3**
Parameters of the nine comparative models in Case one.

| Models | Parameters |
|---|---|
| *DGSTPM* | $\widehat{\eta} = 0.973$, $\widehat{\xi} = 350.008$, $\widehat{\sigma}_1 = 19619.321$, $\widehat{\sigma}_2 = 19542.817$, $\widehat{\sigma}_3 = 19661.537$, $\widehat{\sigma}_4 = 19459.560$, $\widehat{\sigma}_5 = 19520.719$, $\widehat{\sigma}_6 = 19972.849$, $\widehat{\sigma}_7 = 19903.937$, $\widehat{\sigma}_8 = 20208.513$, $\widehat{\sigma}_9 = 19693.671$, $\widehat{\sigma}_{10} = 19852.919$, $\widehat{\sigma}_{11} = 19835.154$, $\widehat{\sigma}_{12} = 19829.938$, $\widehat{\gamma} = 1.085$ |
| *DGSTM* | $\widehat{\alpha} = 1.026$, $\widehat{\beta} = -485.895$, $\widehat{\gamma}_1 = 18569.236$, $\widehat{\gamma}_2 = 18596.280$, $\widehat{\gamma}_3 = 18706.021$, $\widehat{\gamma}_4 = 18491.571$, $\widehat{\gamma}_5 = 18552.986$, $\widehat{\gamma}_6 = 19003.503$, $\widehat{\gamma}_7 = 18910.304$, $\widehat{\gamma}_8 = 19195.755$, $\widehat{\gamma}_9 = 18646.991$, $\widehat{\gamma}_{10} = 18800.925$, $\widehat{\gamma}_{11} = 18770.091$, $\widehat{\gamma}_{12} = 18753.481$ |
| *SARIMA* | $SARIMA(1,1,2)(0,1,0)_{12}$, $AR(1) = -0.61^{***}$,$MA(2) = -0.37^{***}$, $AIC = -4.87$, $LogL = 234.78$ |
| *BPNN* | Embedding dimension $m \in [8, 15]$, time lag $\tau \in [1, 2]$, optimal $m = 13$, optimal, a single hidden layer, the number of neuros $= 14$, and the epochs iteration $= 1000$. |
| *SGM* | $\widehat{\alpha}_s = [-0.001, 18506.119]$, $f_s(1) = 0.986$, $f_s(2) = 0.988$, $f_s(3) = 0.994$, $f_s(4) = 0.984$, $f_s(5) = 0.988$, $f_s(6) = 1.012$, $f_s(7) = 1.008$, $f_s(8) = 1.024$, $f_s(9) = 0.997$, $f_s(10) = 1.006$, $f_s(11) = 1.006$, $f_s(12) = 1.006$ |
| *LSSVM* | Embedding dimension $m \in [8, 15]$, time lag $\tau \in [1, 2]$, optimal $m = 12$, optimal $\tau = 1$, the linear kernel $K(x, y) = x^T y$, penalty parameter $\gamma \in [0.001, 3633.811]$,the optimal $\gamma = 0.165$. |
| *LSTM* | Embedding dimension $m \in [8, 15]$, time lag $\tau \in [1, 2]$, optimal $m = 12$, optimal $\tau = 1$, optimizers = Adam, learning rate = 0.001, decay = 1e-6, two hidden layers, the number of neurons in the first and second layer = 8 and 4, loss='mean_squared_error', epochs = 100, batch size = 1. |
| *SDTGM* | $SARIMA(4,1,2)(0,1,0)_{12}$, $AR(4) = -0.301^{***}$,$MA(1) = -0.571^{***}$, $AIC = -4.99$, $LogL = 240.35$<br>GM(1,1):$\widehat{\alpha} = [-0.0011, 18356.04]$ (Last rolling sample). |
| *FTGM* | $\widehat{\theta} = [0.00067, 18603.1, -0.000016, -0.000019, 0.000096, -0.000053, -50.57, -169.3, -43.4, 132.2]$ |

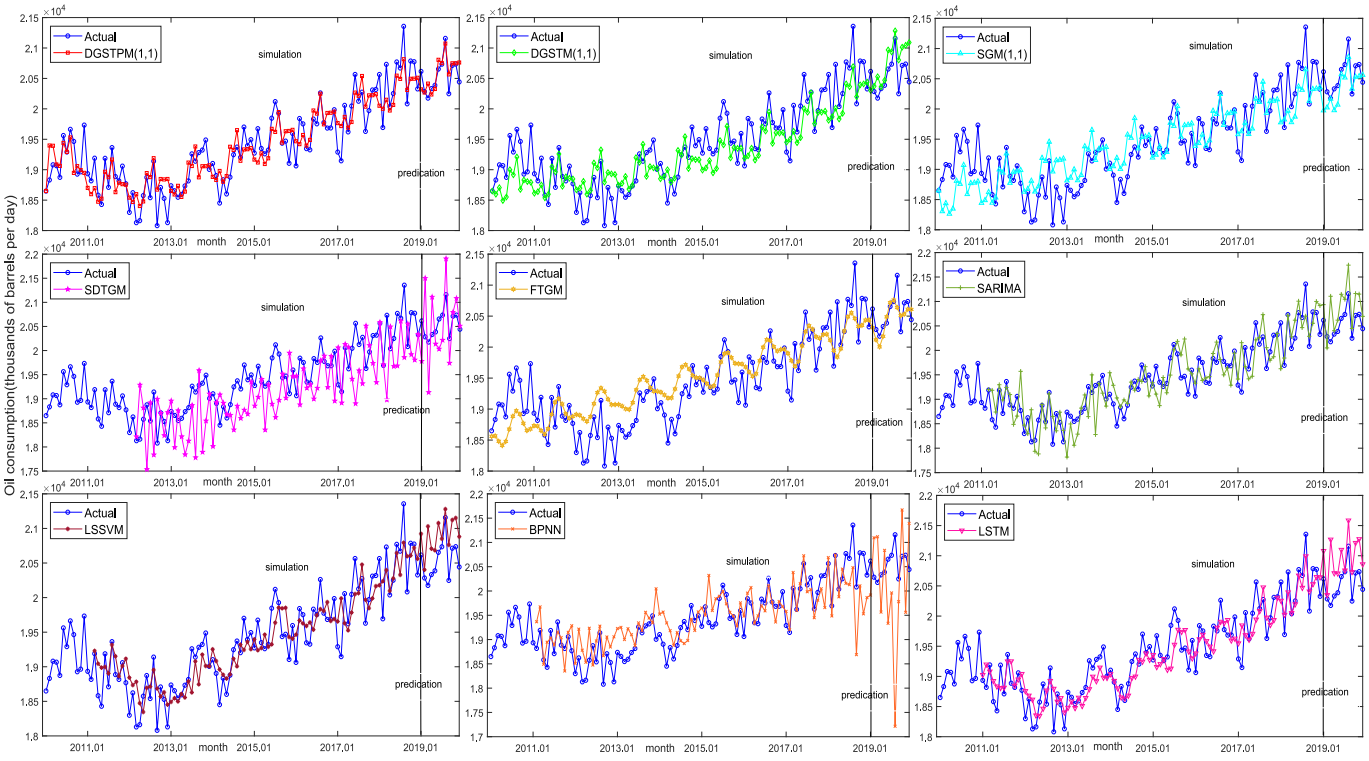


**Fig. 3.** The simulation and forecast results of the nine competing models in Case one.

**Table 4**
The forecasted results and errors of nine models in Case one.

| Month | Actual | *DGSTPM* | *APE* | *DGSTM* | *APE* | *SGM* | *APE* | *SDTGM* | *APE* | *FTGM* | *APE* | *SARIMA* | *APE* | *LSSVM* | *APE* | *BPNN* | *APE* | *LSTM* | *APE* |
|---|---|---|---|---|---|---|---|---|---|---|---|---|---|---|---|---|---|---|---|
| **2019.M1** | 20614.98 | 20319.71 | 1.43 | 20302.24 | 1.52 | 19974.97 | 3.10 | 19778.33 | 4.06 | 20313.12 | 1.46 | 20935.39 | 1.55 | 20921.77 | 1.49 | 19916.41 | 3.39 | 21080.60 | 2.26 |
| **2019.M2** | 20283.87 | 20268.71 | 0.07 | 20372.90 | 0.44 | 20023.41 | 1.28 | 21500.70 | 6.00 | 20116.81 | 0.82 | 20050.49 | 1.15 | 20402.26 | 0.58 | 21095.71 | 4.00 | 20347.79 | 0.32 |
| **2019.M3** | 20176.24 | 20414.72 | 1.18 | 20528.11 | 1.74 | 20168.71 | 0.04 | 19132.91 | 5.17 | 20003.88 | 0.85 | 21106.11 | 4.61 | 21030.71 | 4.24 | 21116.98 | 4.66 | 21268.91 | 5.42 |
| **2019.M4** | 20332.60 | 20236.59 | 0.47 | 20363.17 | 0.15 | 19977.72 | 1.75 | 21110.07 | 3.82 | 20174.14 | 0.78 | 20401.47 | 0.34 | 20706.83 | 1.84 | 19565.79 | 3.77 | 20710.99 | 1.86 |
| **2019.M5** | 20387.09 | 20326.76 | 0.30 | 20469.79 | 0.41 | 20070.43 | 1.55 | 20137.64 | 1.22 | 20487.93 | 0.49 | 20617.71 | 1.13 | 20683.81 | 1.46 | 20836.32 | 2.20 | 20706.89 | 1.57 |
| **2019.M6** | 20653.98 | 20805.94 | 0.74 | 20968.30 | 1.52 | 20573.86 | 0.39 | 20032.98 | 3.01 | 20716.97 | 0.30 | 21146.46 | 2.38 | 21077.22 | 2.05 | 19334.19 | 6.39 | 21099.10 | 2.16 |
| **2019.M7** | 20734.57 | 20751.78 | 0.08 | 20936.09 | 0.97 | 20519.39 | 1.04 | 20217.52 | 2.49 | 20758.92 | 0.12 | 21045.60 | 1.50 | 20849.89 | 0.56 | 19959.64 | 3.74 | 20757.31 | 0.11 |
| **2019.M8** | 21157.91 | 21072.96 | 0.40 | 21281.70 | 0.59 | 20861.23 | 1.40 | 21905.40 | 3.53 | 20638.67 | 2.45 | 21742.83 | 2.76 | 21279.45 | 0.57 | 17215.06 | 18.64 | 21585.36 | 2.02 |
| **2019.M9** | 20248.48 | 20566.61 | 1.57 | 20802.10 | 2.73 | 20333.90 | 0.42 | 19741.59 | 2.50 | 20508.34 | 1.28 | 20446.42 | 0.98 | 20761.55 | 2.53 | 19780.54 | 2.31 | 20732.38 | 2.39 |
| **2019.M10** | 20713.99 | 20748.22 | 0.17 | 21012.69 | 1.44 | 20531.82 | 0.88 | 20792.20 | 0.38 | 20531.66 | 0.88 | 21162.17 | 2.16 | 21122.48 | 1.97 | 21668.77 | 4.61 | 21213.94 | 2.41 |
| **2019.M11** | 20736.15 | 20748.41 | 0.06 | 21044.01 | 1.48 | 20539.96 | 0.95 | 21083.32 | 1.67 | 20609.61 | 0.61 | 21150.36 | 2.00 | 21151.17 | 2.00 | 19560.57 | 5.67 | 21275.63 | 2.60 |
| **2019.M12** | 20442.87 | 20761.55 | 1.56 | 21090.36 | 3.17 | 20562.87 | 0.59 | 20509.82 | 0.33 | 20607.47 | 0.81 | 20695.55 | 1.24 | 20880.66 | 2.14 | 21390.98 | 4.64 | 20859.56 | 2.04 |
| ***MAPES*** | | | 1.19 | | 1.51 | | 1.62 | | 2.97 | | 1.77 | | 1.65 | | 1.30 | | 1.76 | | 1.26 |
| ***MAPEP*** | | | 0.67 | | 1.35 | | 1.12 | | 2.85 | | 0.91 | | 1.82 | | 1.79 | | 5.33 | | 2.10 |
| ***RMSES*** | | | 289.50 | | 358.65 | | 395.73 | | 732.80 | | 420.06 | | 394.59 | | 312.13 | | 436.25 | | 295.71 |
| ***RMSEP*** | | | 180.70 | | 329.37 | | 279.56 | | 679.19 | | 223.99 | | 431.72 | | 415.09 | | 1417.80 | | 499.20 |

**Table 5**
Parameters of the nine competing models in Case two.

| Models | Parameters |
|---|---|
| *DGSTPM* | $\widehat{\eta}=0.9875,\quad \widehat{\xi}=0.843,\quad \widehat{\sigma}_1=11981.094,\quad \widehat{\sigma}_2=12605.186,$ $\widehat{\sigma}_3=12591.354,\ \widehat{\sigma}_4=12474.757,\quad \widehat{\gamma}=2.499$ |
| *DGSTM* | $\widehat{\alpha}=0.846,\quad \widehat{\beta}=1704.295,\quad \widehat{\gamma}_1=11774.643,$ $\widehat{\gamma}_2=18596.280,\quad \widehat{\gamma}_3=12376.740,\quad \widehat{\gamma}_4=12358.015$ |
| *SARIMA* | $SARIMA(4,1,0)(0,1,0)_4,\quad AR(4)=-0.70^{***}, AIC=-3.33, LogL=40.32$ |
| *BPNN* | Embedding dimension $m\in[3,15]$, time lag $\tau\in[1,2]$, optimal $m=7$, optimal $\tau=1$, a single hidden layer, the number of neuros = 5, the epochs iteration = 1000. |
| *SGM* | $\widehat{\alpha}_s=[0.002,11706.59],\ f_s(1)=0.961,\ f_s(2)=1.019,\ f_s(3)=1.016,$ $f_s(4)=1.004$ |
| *LSSVM* | Embedding dimension $m\in[3,15]$, time lag $\tau\in[1,2]$, optimal $m=12$, optimal $\tau=1$, Linear kernel $K(x,y)=x^Ty, \gamma\in[0.002,6457.825]$,optimal $\gamma=0.293$. |
| *LSTM* | Embedding dimension $m\in[3,15]$, time lag $\tau\in[1,2]$, optimal $m=4$, optimal $\tau=1$, optimizers = Adam, learning rate = 0.001, decay = 1e-6, two hidden layers, the number of neurons in the first and second layer = 4 and 4, loss='mean_squared_error', epochs = 100, batch_size = 1. |
| *SDTGM* | $SARIMA(4,1,0)(0,1,0)_4,\ AR(4)=-0.661^{***},\quad AIC=-3.19,$ $LogL=38.76$ GM(1,1):$\widehat{\alpha}=[-0.00034,11295.59]$ (Last rolling sample). |
| *FTGM* | $\widehat{\theta}=[-0.0053,12106.5,0.00011,-0.00096,-15.28,-194.18]$ |

Note: the***indicates the *p*-value of the corresponding parameter is less than 0.01.

$$\widehat{s}^{(0)}(t)=\widehat{\eta}^{t-2}(\widehat{\eta}-1)s^{(0)}(1)+\sum_{a=2}^{t-1}\widehat{\eta}^{t-1-a}(a^{\gamma}-(a-1)^{\gamma})\widehat{\xi}+\widehat{\eta}^{t-2}\widehat{\xi}+\widehat{\eta}^{t-2}\widehat{\sigma}_2+\sum_{a=3}^{t}\widehat{\eta}^{t-a}\left(\widehat{\sigma}_{M(a,c)}-\widehat{\sigma}_{M(a-1,c)}\right) \tag{13}$$

Subsequently, the cumulative generation sequence is obtained:

$$\begin{aligned}\widehat{s}^{(1)}(t)&=\sum_{i=1}^{t}\widehat{s}^{(0)}(i)=\widehat{s}^{(0)}(1)+\widehat{s}^{(0)}(2)+\widehat{s}^{(0)}(3)+\ldots+\widehat{s}^{(0)}(t-1)+\widehat{s}^{(0)}(t)\\&=s^{(0)}(1)+(\widehat{\eta}-1)s^{(0)}(1)+\widehat{\xi}+\widehat{\sigma}_2+\widehat{\eta}(\widehat{\eta}-1)s^{(0)}(1)+(2^{\gamma}-1)\widehat{\xi}+\widehat{\eta}\widehat{\xi}\\&\quad+\widehat{\eta}\widehat{\sigma}_2+\widehat{\sigma}_3-\widehat{\sigma}_2\ldots+\widehat{\eta}^{t-3}(\widehat{\eta}-1)s^{(0)}(1)+\sum_{a=2}^{t-2}\widehat{\eta}^{t-2-a}(a^{\gamma}-(a-1)^{\gamma})\widehat{\xi}\\&\quad+\widehat{\eta}^{t-3}\widehat{\xi}+\widehat{\eta}^{t-3}\widehat{\sigma}_2+\sum_{a=3}^{t-1}\widehat{\eta}^{t-1-a}\left(\widehat{\sigma}_{M(a,c)}-\widehat{\sigma}_{M(a-1,c)}\right)\\&\quad+\widehat{\eta}^{t-2}(\widehat{\eta}-1)s^{(0)}(1)+\sum_{a=2}^{t-1}\widehat{\eta}^{t-1-a}(a^{\gamma}-(a-1)^{\gamma})\widehat{\xi}+\widehat{\eta}^{t-2}\widehat{\xi}+\widehat{\eta}^{t-2}\widehat{\sigma}_2\\&\quad+\sum_{a=3}^{t}\widehat{\eta}^{t-a}\left(\widehat{\sigma}_{M(a,c)}-\widehat{\sigma}_{M(a-1,c)}\right)\\&=\widehat{\eta}^{t-1}s^{(0)}(1)+\sum_{a=1}^{t-1}\widehat{\eta}^{t-1-a}a^{\gamma}\widehat{\xi}+\widehat{\eta}^{t-2}\widehat{\sigma}_2+\sum_{a=3}^{t}\widehat{\eta}^{t-a}\widehat{\sigma}_{M(a,c)}\end{aligned} \tag{14}$$

Similarity, we can get

$$\widehat{s}^{(1)}(t+1)=\widehat{\eta}^{t}s^{(0)}(1)+\sum_{a=1}^{t}\widehat{\eta}^{t-a}a^{\gamma}\widehat{\xi}+\widehat{\eta}^{t-1}\widehat{\sigma}_2+\sum_{a=3}^{t+1}\widehat{\eta}^{t+1-a}\widehat{\sigma}_{M(a,c)} \tag{15}$$

Hence ,

$$\widehat{s}^{(1)}(t+1)=\widehat{\eta}s^{(1)}(t)+\widehat{\xi}t^{\gamma}+\widehat{\sigma}_{M(t+1,c)} \tag{16}$$

Based on Theorem 1 and Theorem 2, We get the simulation of the $\widehat{\widehat{s}}^{(1)}(t)$ and $\widehat{\widehat{s}}^{(0)}(t)$.

$$\widehat{\widehat{s}}^{(1)}(t)=\widehat{\eta}^{t-1}s^{(0)}(1)+\sum_{a=1}^{t-1}\widehat{\eta}^{t-1-a}a^{\gamma}\widehat{\xi}+\widehat{\eta}^{t-2}\widehat{\sigma}_2+\sum_{a=3}^{t}\widehat{\eta}^{t-a}\widehat{\sigma}_{M(a,c)} \tag{17}$$

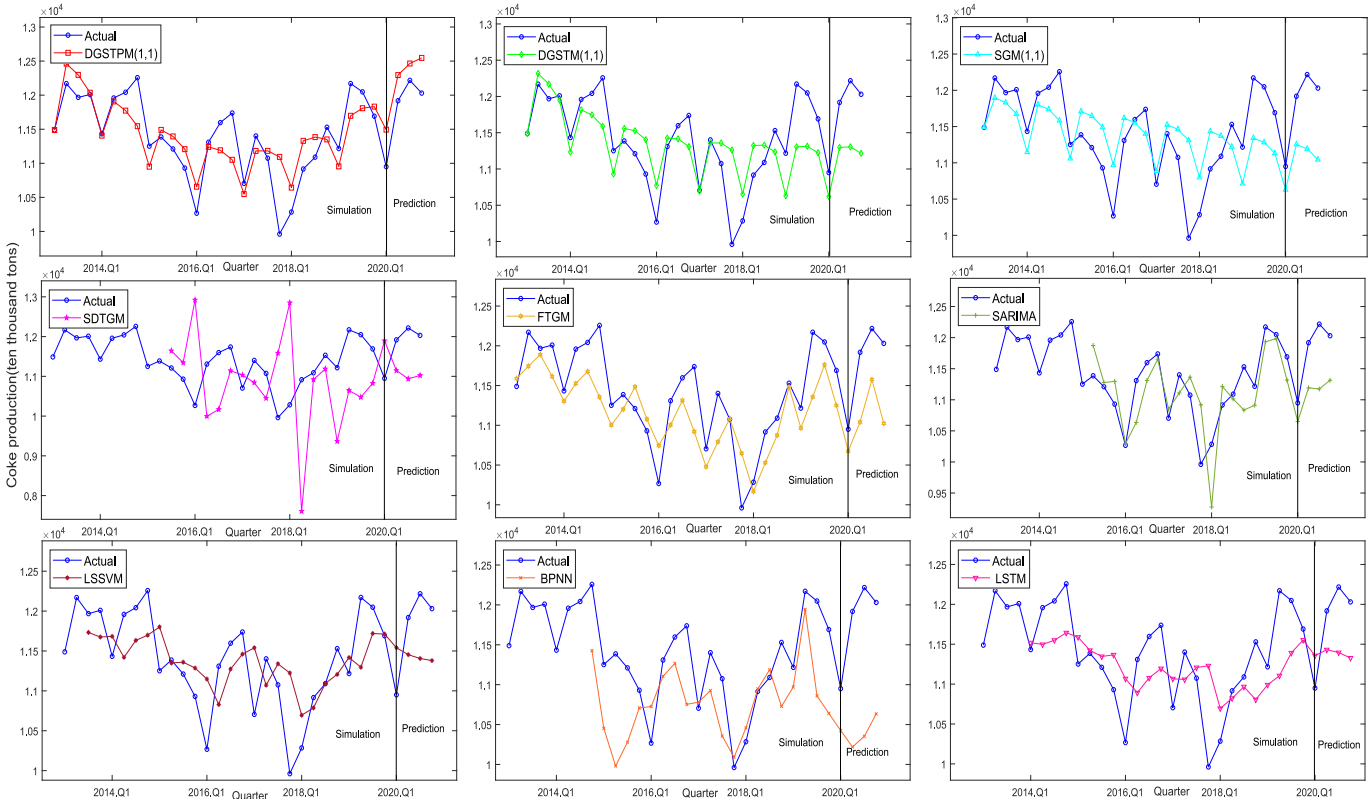


**Fig. 4.** The simulation and forecast curves of the nine competing models in Case two.

$$\widehat{\widehat{s}}^{(0)}(t)=\widehat{\eta}^{t-2}(\widehat{\eta}-1)s^{(0)}(1)+\sum_{a=2}^{t-1}\widehat{\eta}^{t-1-a}(a^{\gamma}-(a-1)^{\gamma})\widehat{\xi}+\widehat{\eta}^{t-2}\widehat{\xi}+\widehat{\eta}^{t-2}\widehat{\sigma}_2+\sum_{a=3}^{t}\widehat{\eta}^{t-a}\left(\widehat{\sigma}_{M(a,c)}-\widehat{\sigma}_{M(a-1,c)}\right),t\geqslant 2 \tag{18}$$

According to Eq. (13) and Eq. (18), the equation $\widehat{\widehat{s}}^{(0)}(t)=\widehat{s}^{(0)}(t),t=1,2,\cdots,n$ can be obtained. Therefore, the *DGSTPM(1,1)*model is unbiased for the seasonal series.

**Property 3.** *Assuming that the original time sequences* $\boldsymbol{S^{(0)}}=\left(s^{(0)}(1),s^{(0)}(2),...,s^{(0)}(n)\right)$ *is collected, whose expression is* $s^{(0)}(t)=(t-1)^{\gamma}\widehat{\xi}+H_{M(t,c)}$, *we will have* $\widehat{\eta}=1,\widehat{\xi}=\xi,\widehat{\sigma}_i=H_{M(i,c)}=H_i,i=1,2,...,c$, *and* $\widehat{s}^{(0)}(t)=s^{(0)}(t)$.

***Proof.*** *As* $s^{(0)}(t)=(t-1)^{\gamma}\widehat{\xi}+H_{M(t,c)}$ , *the seasonal sequence* $\boldsymbol{S^{(0)}}$ *can be obtained by* $\boldsymbol{S^{(0)}}=\left(H_1,\widehat{\xi}+H_2,...,\widehat{\xi}(c-1)^{\gamma}+H_c,\widehat{\xi}c^{\gamma}+H_1,\cdots,H_1,H_2,...,\widehat{\xi}(n-1)^{\gamma}+H_{M(n,c)}\right)$ *when* t mod c $=0$,

$$\begin{cases} s^{(1)}(t)=\sum_{a=0}^{t-1}a^{\gamma}\widehat{\xi}+\frac{t}{c}\sum_{i=1}^{c}H_i \\ s^{(1)}(t+1)=\sum_{a=0}^{t}a^{\gamma}\widehat{\xi}+\frac{t}{c}\sum_{i=1}^{c}\sigma_i+H_1 \end{cases} \tag{19}$$

We can get $s^{(1)}(t+1)=s^{(1)}(t)+\xi t^{\gamma}+\sigma_1=s^{(1)}(t)+\xi t^{\gamma}+\sigma_{M(t+1,c)}$. When t mod c $\neq 0$, we will obtain

$$\begin{cases} s^{(1)}(t)=\sum_{a=0}^{t-1}a^{\gamma}\xi+\frac{(t-M(t,c))}{c}\sum_{i=1}^{c}H_i+\sum_{i=1}^{M(t,c)}H_i \\ s^{(1)}(t+1)=\sum_{a=0}^{t}a^{\gamma}\xi+\frac{(t+1-M(t+1,c))}{c}\sum_{i=1}^{c}H_i+\sum_{i=1}^{M(t+1,c)}H_i \end{cases} \tag{20}$$

According to Eq. (18) and $M(t+1,c)=M(t,c)+1$, we can possess

$$s^{(1)}(t+1)=s^{(1)}(t)+\xi t^{\gamma}+H_{M(t+1,c)} \tag{21}$$

$$=\widehat{\eta}s^{(1)}(t)+\widehat{\xi}t^{\gamma}+\widehat{\sigma}_{M(t+1,c)} \tag{22}$$

So, $\widehat{\eta}=1,\widehat{\xi}=\xi,\widehat{\sigma}_i=H_{M(i,c)}=H_i$. The property 3 is proofed.

As many sequences are characterized by nonlinear tendency and periodic fluctuations in practice, such as oil consumption, the proposed model can provide an improved approach for analyzing sequences based on Property 3. Empirical studies involving two cases further demonstrate the applicability of Property 3, thereby establishing the validity and universality of this novel model.

**Property 4.** *Based on the obtained time series* $S^{(0)}$, *the relationship between* $\widehat{s}^{(0)}(t+c)$ *and* $\widehat{s}^{(0)}(t)$ *of the proposed DGSTPM(1,1) model can be obtained.*

$$\widehat{s}^{(0)}(t+c)=\widehat{\eta}^{c}\widehat{s}^{(0)}(t)+\sum_{a=t}^{t+c-1}\widehat{\eta}^{t+c-1-a}(a^{\gamma}-(a-1)^{\gamma})\widehat{\xi}+\psi_{M(t,c)},t\geqslant 2 \tag{23}$$

where

**Table 6**
The forecasted results, APE(%), MAPE(%), and RMSE for the six models in Case two.

| Quarter | Actual | *DGSTPM* | *APE* | *DGSTM* | *APE* | *SGM* | *APE* | *SDTGM* | *APE* | *FTGM* | *APE* | *SARIMA* | *APE* | *LSSVM* | *APE* | *BPNN* | *APE* | *LSTM* | *APE* |
|---|---|---|---|---|---|---|---|---|---|---|---|---|---|---|---|---|---|---|---|
| **2020.Q1** | 10950.40 | 11493.83 | 4.96 | 10620.79 | 3.01 | 10629.21 | 2.93 | 11894.83 | 8.62 | 10675.19 | 2.51 | 10651.23 | 2.73 | 11540.89 | 5.39 | 10425.23 | 4.80 | 11356.70 | 3.71 |
| **2020.Q2** | 11918.20 | 12294.61 | 3.16 | 11296.59 | 5.22 | 11253.51 | 5.58 | 11146.32 | 6.48 | 11041.01 | 7.36 | 11192.05 | 6.09 | 11453.58 | 3.90 | 10219.75 | 14.25 | 11431.29 | 4.09 |
| **2020.Q3** | 12217.20 | 12464.46 | 2.02 | 11305.77 | 7.46 | 11192.73 | 8.39 | 10937.91 | 10.47 | 11574.62 | 5.26 | 11173.97 | 8.54 | 11405.68 | 6.64 | 10353.42 | 15.26 | 11395.85 | 6.72 |
| **2020.Q4** | 12030.30 | 12546.70 | 4.29 | 11216.33 | 6.77 | 11044.23 | 8.20 | 11022.16 | 8.38 | 11024.41 | 8.36 | 11314.33 | 5.95 | 11379.15 | 5.41 | 10633.51 | 11.61 | 11327.32 | 5.84 |
| ***MAPES*** | | | 2.58 | | 3.12 | | 3.63 | | 11.20 | | 3.01 | | 3.23 | | 3.57 | | 4.73 | | 3.87 |
| ***MAPEP*** | | | 3.61 | | 5.61 | | 6.27 | | 8.49 | | 5.87 | | 5.83 | | 5.34 | | 11.48 | | 5.09 |
| ***RMSES*** | | | 375.00 | | 449.97 | | 491.71 | | 1520.52 | | 417.06 | | 453.85 | | 492.67 | | 677.00 | | 531.06 |
| ***RMSEP*** | | | 437.26 | | 705.03 | | 801.07 | | 1017.43 | | 753.31 | | 744.60 | | 641.70 | | 1465.03 | | 626.69 |

$$\begin{cases} \psi_1 = \widehat{\eta}^{c-1}(\widehat{\sigma}_2 - \widehat{\sigma}_1) + \widehat{\eta}^{c-2}(\widehat{\sigma}_3 - \widehat{\sigma}_2) + \cdots + \widehat{\eta}(\widehat{\sigma}_c - \widehat{\sigma}_{c-1}) + \widehat{\sigma}_1 - \widehat{\sigma}_c \\ \psi_2 = \widehat{\eta}^{c-1}(\widehat{\sigma}_3 - \widehat{\sigma}_2) + \widehat{\eta}^{c-2}(\widehat{\sigma}_4 - \widehat{\sigma}_3) + \ldots + \widehat{\eta}(\widehat{\sigma}_1 - \widehat{\sigma}_c) + \widehat{\sigma}_2 - \widehat{\sigma}_1 \\ \vdots \\ \psi_c = \widehat{\eta}^{c-1}(\widehat{\sigma}_1 - \widehat{\sigma}_c) + \widehat{\eta}^{c-2}(\widehat{\sigma}_2 - \widehat{\sigma}_1) + \ldots + \widehat{\eta}(\widehat{\sigma}_{c-1} - \widehat{\sigma}_{c-2}) + \widehat{\sigma}_c - \widehat{\sigma}_{c-1} \end{cases} \tag{24}$$

**Proof.** According to theorem 2, the following formula can be obtained,

$$\widehat{s}^{(0)}(t) = \widehat{\eta}^{t-2}(\widehat{\eta}-1)s^{(0)}(1) + \sum_{a=2}^{t-1}\widehat{\eta}^{t-1-a}(a^{\gamma}-(a-1)^{\gamma})\widehat{\xi} + \widehat{\eta}^{t-2}\widehat{\xi} + \widehat{\eta}^{t-2}\widehat{\sigma}_2 + \sum_{a=3}^{t}\widehat{\eta}^{t-a}\left(\widehat{\sigma}_{M(a,c)} - \widehat{\sigma}_{M(a-1,c)}\right) \tag{25}$$

and

$$\widehat{s}^{(0)}(t+c) = \widehat{\eta}^{t+c-2}(\widehat{\eta}-1)s^{(0)}(1) + \widehat{\eta}^{t+c-2}\widehat{\xi} + \sum_{a=2}^{t+c-1}\widehat{\eta}^{t+c-a-1}(a^{\gamma}-(a-1)^{\gamma})\widehat{\xi} + \widehat{\eta}^{t+c-2}\widehat{\sigma}_2 + \sum_{a=3}^{t+c}\widehat{\eta}^{t+c-a}\left(\widehat{\sigma}_{M(a,c)} - \widehat{\sigma}_{M(a-1,c)}\right) \tag{26}$$

Adding $\widehat{\eta}^{c}$ to both sides of Eq. (25), we can get

$$\eta^{c}\widehat{s}^{(0)}(t) = \widehat{\eta}^{t+c-2}(\widehat{\eta}-1)s^{(0)}(1) + \widehat{\eta}^{c}\widehat{\eta}^{t-2}\widehat{\xi} + \sum_{a=2}^{t-1}\widehat{\eta}^{t+c-1-a}(a^{\gamma}-(a-1)^{\gamma})\widehat{\xi} + \sum_{a=3}^{t}\widehat{\eta}^{t+c-a}\left(\widehat{\sigma}_{M(a,c)} - \widehat{\sigma}_{M(a-1,c)}\right) \tag{27}$$

Analyzing Eq. (26) and Eq. (27), we will have

$$\widehat{s}^{(0)}(t+c) = \widehat{\eta}^{c}\widehat{s}^{(0)}(t) + \sum_{a=t}^{t+c-1}\widehat{\eta}^{t+c-1-a}(a^{\gamma}-(a-1)^{\gamma})\widehat{\xi} + \sum_{a=t+1}^{t+c}\widehat{\eta}^{t+c-a}\left(\widehat{\sigma}_{M(a,c)} - \widehat{\sigma}_{M(a-1,c)}\right) \tag{28}$$

where $\sum_{a=t+1}^{t+c}\widehat{\eta}^{t+c-a}\left(\widehat{\sigma}_{M(a,c)} - \widehat{\sigma}_{M(a-1,c)}\right)$ can be used as a complete cycle of the seasonal sequence. When $t = 2$, the seasonal factor in the formula is expressed as follows

$$\begin{aligned} \psi_2 = \psi_{M(2,c)} &= \sum_{a=2+1}^{2+c}\widehat{\eta}^{2+c-a}\left(\widehat{\sigma}_{M(a,c)} - \widehat{\sigma}_{M(a-1,c)}\right) \\ &= \widehat{\eta}^{c-1}(\widehat{\sigma}_3 - \widehat{\sigma}_2) + \widehat{\eta}^{c-2}(\widehat{\sigma}_4 - \widehat{\sigma}_3) + \ldots + \widehat{\eta}(\widehat{\sigma}_1 - \widehat{\sigma}_c) + \widehat{\sigma}_2 - \widehat{\sigma}_1 \end{aligned} \tag{29}$$

For $t = 3, 4, \cdots c, c+1$, We can get $\psi_{M(t,c)}$ in the same way.

Drawing upon Property 4, we delve into the inner workings of the novel model, elucidating the apparent correlation between $\widehat{s}^{(0)}(t+c)$ and $\widehat{s}^{(0)}(t)$. Consequently, in practical applications, embracing or rejecting the model hinges on an insightful analysis of the rules concealed within $s^{(0)}(t+c)$ and $s^{(0)}(t)$.

## 3. Empirical studies

This section employs two energy-related cases with diverse sample sizes and data characteristics to further validate the model's effectiveness and applicability, including monthly oil consumption in the United States and quarterly coke production in China, compared with a series of classic prediction models. Specifically, we elaborated on the experimental design, data collection, and comparative models in Section 3.1. The parameter estimation of different models is presented in Section 3.2. In Section 3.3, evaluation criteria for predicting models are provided. Next, Section 3.4 focuses on the comparisons of nine competing models in two empirical studies. Specifically, *DGSTPM(1,1)*, *DGSTM(1,1)*,

**Table 7**
The *DM* test results for *DGSTPM(1,1)* as the benchmark model.

| | | | *DGSTM* | *SGM* | *SDTGM* | *FTGM* | *SARIMA* | *LSSVM* | *BPNN* | *LSTM* |
|---|---|---|---|---|---|---|---|---|---|---|
| Case one: | *APE* | *DW* | −4.767 | −5.125 | −3.998 | −5.071 | −3.89 | −2.271 | −2.286 | −1.899 |
| Monthly oil consumption | | *p* | **5.3E-06** | **1.1E-06** | **1.2E-04** | **1.4E-06** | **1.7E-04** | **0.025** | **0.024** | **0.060** |
| | *SE* | *DW* | −3.844 | −3.946 | −2.914 | −3.15 | −3.082 | −1.818 | −1.078 | −1.331 |
| | | *p* | **1.9E-04** | **1.3E-04** | **0.0045** | **2.0E-03** | **0.003** | **0.071** | 0.283 | 0.185 |
| Case two: | *APE* | *DW* | −2.376 | −3.079 | −3.001 | −1.128 | −1.086 | −1.435 | −2.496 | −2.880 |
| Quarterly coke production | | *p* | **2.3E-02** | **4.3E-03** | **0.006** | 0.267 | 0.289 | 0.161 | **0.019** | **0.007** |
| | *SE* | *DW* | −2.027 | −2.232 | −1.913 | −0.738 | −1.054 | −2.227 | −2.129 | −2.184 |
| | | *p* | **0.051** | **0.033** | **0.069** | 0.465 | 0.303 | **0.033** | **0.043** | **0.037** |

*STDGM, FTGM, SARIMA*, *BPNN*, *SGM(1,1)*, *LSSVM,* and *LSTM* models are used to effectively describe the periodicity and complexity of the two selected sequences, respectively. Comparisons of nine prediction models over the DM, and SPA tests are shown in Section 3.5. Lastly, several conclusions will be drawn from the two case studies in Section 3.6.

### 3.1. Experimental design, data collection, and comparative models

To assess the validity of the *DGSTPM(1,1)* model, this paper conducts a comprehensive multi-model experiment for forecasting two cases. The study introduces eight representative comparative models to validate the new model's effectiveness in practical forecasting. These models are categorized into three groups: the grey (or grey hybrid) prediction model (*DGSTM(1,1), SGM(1,1), SDTGM,* and *FTGM*), the traditional econometric model (*SARIMA*), and artificial intelligence models (*BPNN, LSSVM,* and *LSTM*). Among the prediction models, *SGM(1,1)* is a classical grey model designed for seasonal series forecasting, and the new model serves as an extension of *DGSTM(1,1)*. *SARIMA* Damp Trend Grey Forecasting Model (*STDGM*) and Fourier Time-Varying Grey Model (*FTGM*) are two grey hybrid models seamlessly integrating grey forecasting with other techniques. The *SARIMA* model represents a typical econometric method, while the *BPNN* and the *LSSVM* models are exemplary artificial intelligence models. *LSTM* stands out as a deep learning model specifically tailored for processing time series data.

Moreover, it is worth noting that all the primary data in the two case studies are gathered from authoritative and official sources. To be more precise, the EPS (Express Professional Superior) furnishes comprehensive information on total oil consumption in the United States, accessible at https://olap.epsnet.com.cn/. Furthermore, data related to China's coke production can be sourced from the China Economic Net Database, which can be accessed through https://db.cei.cn/.

### 3.2. Parameter estimation

We employ the iterative optimization of the cultural algorithm to get the parameter of the time power index. The ordinary parameters of the new and other four grey (or grey hybrid) prediction models, including *DGSTM(1,1)*, *SGM(1,1)*, the *GM(1,1)* component within *SDTGM*, and *FTGM* are determined by applying the *OLS* technique. For the *SARIMA* model and the *SARIMA* component within *STDGM*, the autocorrelation and partial correlation orders are determined by *ACF* and *PACF*, respectively. The corresponding coefficients are derived by using the maximum likelihood function. And the optimal form is determined based on the Akaike Information Criterion (*AIC*). In the LSSVM model, the kernel function adopts the Gaussian kernel function $K(x,y) = e^{-\|x-y\|^2/2\sigma^2}$ or the Linear kernel function $K(x,y) = x^T y$. Additionally, for the *BPNN*, *LSSVM*, and *LSTM* models, the embedding dimension and delay time are selected using the grid search method.

### 3.3. Evaluation criteria for predicting models

Evaluation criteria play a crucial role in assessing the performance of various prediction models. In this paper, the following five evaluation criteria are adopted to analyze the model results: absolute percentage error (*APE*), mean absolute percentage error of simulation and prediction (*MAPES* and *MAPEP*), square error (*SE*), and root mean square error of simulation and prediction (*RMSES* and *RMSEP*). The five evaluation criteria are as follows,

$$\mathrm{APE}(t) = \left|\frac{\hat{s}^{(0)}(t) - s^{(0)}(t)}{s^{(0)}(t)}\right| \times 100\%, \quad t = 1, 2, \cdots, n+h \tag{30}$$

$$\mathrm{MAPES} = \frac{1}{n}\sum_{t=1}^{n}\mathrm{APE}(t), \quad \mathrm{MAPEP} = \frac{1}{h}\sum_{t=n+1}^{n+h}\mathrm{APE}(t) \tag{31}$$

$$SE(t) = \left(\hat{s}^{(0)}(t) - s^{(0)}(t)\right)^2 \tag{32}$$

$$\begin{aligned}\mathrm{RMSES} &= \sqrt{\frac{1}{n}\sum_{t=1}^{n}\left(\hat{s}^{(0)}(t) - s^{(0)}(t)\right)^2}, \mathrm{RMSEP} \\ &= \sqrt{\frac{1}{h}\sum_{t=n+1}^{n+h}\left(\hat{s}^{(0)}(t) - s^{(0)}(t)\right)^2}\end{aligned} \tag{33}$$

Among the above formulas, $n$ represents the number of training sets, and $h$ is the prediction step. These criteria provide comprehensive metrics to evaluate the accuracy and reliability of the prediction models under consideration.

The corresponding criteria for accuracy classification are presented in Table 2. Additionally, based on Absolute Percentage Error (*APE*) and Square Error (SE), two statistical tests, namely Superior Predictive Ability (*SPA TEST*) and Diebold-Mariandm (DM) tests, are employed in this study to assess the modeling performance of nine models. This serves as a foundation for evaluating the effectiveness and robustness of the new model.

### 3.4. Empirical analysis

#### 3.4.1. Case one: Monthly oil consumption in the United States

Oil serves as a primary energy source, constituting a significant portion of the global energy consumption mix (Hu & Chen, 2023). Given the United States' substantial reliance on oil, accurate predictions play a crucial role in developing rational energy deployment plans and mitigating potential oil security issues. The intricacies of American oil consumption data, marked by seasonal and complex patterns, make it challenging to characterize effectively. To assess the efficacy of *DGSTPM (1,1)*, monthly oil consumption data in the USA from 2010 to 2019 is employed. The dataset with observations from 2010 M1 to 2018 M12 forms the in-sample set for model training. The last 12 monthly data points in 2019 constitute the out-of-sample set for evaluating the predictive performance of nine forecasting models. Our study proposes a method that focuses on predicting monthly oil consumption in the United States, aiming to validate the effectiveness and universality of the model, particularly in forecasting seasonal time series characterized by large sample sizes and intricate fluctuations.

The parameter results of the nine models based on the parameter estimation method are presented in Table 3. Since oil consumption follows a monthly sequence, the new model trains thirteen parameters and one-time power index to provide projections. The optimal form of

**Table 8**
The *SPA* test results for nine prediction models.

| Benchmarks | Case one: Monthly oil consumption | | | | | | | | | Case two: Quarterly coke production | | | | | | | |
|---|---|---|---|---|---|---|---|---|---|---|---|---|---|---|---|---|---|
| | | ***DGSTM*** | ***SGM*** | ***SDTGM*** | ***FTGM*** | ***SARIMA*** | ***LSSVM*** | ***BPNN*** | ***LSTM*** | ***DGSTM*** | ***SGM*** | ***SDTGM*** | ***FTGM*** | ***SARIMA*** | ***LSSVM*** | ***BPNN*** | ***LSTM*** |
| ***DGSTPM*** | *APE* | 1 | 1 | 1 | 1 | 1 | 1 | 1 | 1 | 1 | 1 | 1 | 1 | 1 | 1 | 1 | 1 |
| | *SE* | 1 | 1 | 1 | 1 | 1 | 1 | 1 | 1 | 1 | 1 | 1 | 1 | 1 | 1 | 1 | 1 |
| | | ***DGSTPM*** | ***SGM*** | ***SDTGM*** | ***FTGM*** | ***SARIMA*** | ***LSSVM*** | ***BPNN*** | ***LSTM*** | ***DGSTPM*** | ***SGM*** | ***SDTGM*** | ***FTGM*** | ***SARIMA*** | ***LSSVM*** | ***BPNN*** | ***LSTM*** |
| ***DGSTM*** | *APE* | 0 | 0.0001 | 1 | 0 | 1 | 1 | 1 | 1 | 0 | 1 | 1 | 1 | 1 | 0 | 1 | 0 |
| | *SE* | 0 | 0 | 1 | 0 | 1 | 1 | 1 | 1 | 0 | 1 | 1 | 1 | 1 | 0 | 1 | 0 |
| | | ***DGSTPM*** | ***DGSTM*** | ***SDTGM*** | ***FTGM*** | ***SARIMA*** | ***LSSVM*** | ***BPNN*** | ***LSTM*** | ***DGSTPM*** | ***DGSTM*** | ***SDTGM*** | ***FTGM*** | ***SARIMA*** | ***LSSVM*** | ***BPNN*** | ***LSTM*** |
| ***SGM*** | *APE* | 0 | 1 | 1 | 0.0002 | 1 | 1 | 1 | 1 | 0 | 0 | 1 | 0.0001 | 0 | 0.0001 | 1 | 0 |
| | *SE* | 0 | 1 | 1 | 0.0003 | 1 | 1 | 1 | 1 | 0 | 0 | 1 | 0.0001 | 0.0002 | 0 | 1 | 0 |
| | | ***DGSTPM*** | ***DGSTM*** | ***SGM*** | ***FTGM*** | ***SARIMA*** | ***LSSVM*** | ***BPNN*** | ***LSTM*** | ***DGSTPM*** | ***DGSTM*** | ***SGM*** | ***FTGM*** | ***SARIMA*** | ***LSSVM*** | ***BPNN*** | ***LSTM*** |
| ***SDTGM*** | *APE* | 0 | 0 | 0 | 0 | 0 | 0 | 1 | 0 | 0 | 0 | 0 | 0 | 0 | 0 | 1 | 0 |
| | *SE* | 0 | 0 | 0 | 0 | 0 | 0 | 1 | 0 | 0 | 0 | 0 | 0 | 0 | 0 | 1 | 0 |
| | | ***DGSTPM*** | ***DGSTM*** | ***SGM*** | ***SDTGM*** | ***SARIMA*** | ***LSSVM*** | ***BPNN*** | ***LSTM*** | ***DGSTPM*** | ***DGSTM*** | ***SGM*** | ***SDTGM*** | ***SARIMA*** | ***LSSVM*** | ***BPNN*** | ***LSTM*** |
| ***FTGM*** | *APE* | 0 | 1 | 1 | 1 | 1 | 1 | 1 | 1 | 0 | 0.0001 | 1 | 1 | 0 | 0 | 1 | 0 |
| | *SE* | 0.0003 | 1 | 1 | 1 | 1 | 1 | 1 | 1 | 0 | 0.0001 | 1 | 1 | 0.0001 | 0.0001 | 1 | 0 |
| | | ***DGSTPM*** | ***DGSTM*** | ***SGM*** | ***SDTGM*** | ***FTGM*** | ***LSSVM*** | ***BPNN*** | ***LSTM*** | ***DGSTPM*** | ***DGSTM*** | ***SGM*** | ***SDTGM*** | ***FTGM*** | ***LSSVM*** | ***BPNN*** | ***LSTM*** |
| ***SARIMA*** | *APE* | 0 | 0 | 0 | 1 | 0 | 0.0003 | 1 | 1 | 0 | 0.0001 | 1 | 1 | 1 | 0 | 1 | 0 |
| | *SE* | 0 | 0.0001 | 0 | 1 | 0 | 0.0001 | 1 | 1 | 0 | 0 | 1 | 1 | 1 | 0 | 1 | 0 |
| | | ***DGSTPM*** | ***DGSTM*** | ***SGM*** | ***SDTGM*** | ***FTGM*** | ***SARIMA*** | ***BPNN*** | ***LSTM*** | ***DGSTPM*** | ***DGSTM*** | ***SGM*** | ***SDTGM*** | ***FTGM*** | ***SARIMA*** | ***BPNN*** | ***LSTM*** |
| ***LSSVM*** | *APE* | 0 | 0 | 0 | 1 | 0 | 1 | 1 | 1 | 0 | 1 | 1 | 1 | 1 | 1 | 1 | 0.0001 |
| | *SE* | 0 | 0.0001 | 0 | 1 | 0 | 1 | 1 | 1 | 0 | 1 | 1 | 1 | 1 | 1 | 1 | 0 |
| | | ***DGSTPM*** | ***DGSTM*** | ***SGM*** | ***SDTGM*** | ***FTGM*** | ***SARIMA*** | ***LSSVM*** | ***LSTM*** | ***DGSTPM*** | ***DGSTM*** | ***SGM*** | ***SDTGM*** | ***FTGM*** | ***SARIMA*** | ***LSSVM*** | ***LSTM*** |
| *BPNN* | *APE* | 0 | 0 | 0 | 0 | 0 | 0 | 0 | 0 | 0 | 0 | 0 | 0 | 0 | 0 | 0 | 0 |
| | *SE* | 0 | 0 | 0 | 0 | 0 | 0 | 0 | 0 | 0 | 0 | 0 | 0 | 0 | 0 | 0 | 0 |
| | | ***DGSTPM*** | ***DGSTM*** | ***SGM*** | ***SDTGM*** | ***FTGM*** | ***SARIMA*** | ***LSSVM*** | ***BPNN*** | ***DGSTPM*** | ***DGSTM*** | ***SGM*** | ***SDTGM*** | ***FTGM*** | ***SARIMA*** | ***LSSVM*** | ***BPNN*** |
| *LSTM* | *APE* | 0 | 0 | 0 | 1 | 0 | 0 | 0 | 1 | 0 | 1 | 1 | 1 | 1 | 1 | 1 | 1 |
| | *SE* | 0 | 0 | 0 | 1 | 0 | 0 | 0 | 1 | 0 | 1 | 1 | 1 | 1 | 1 | 1 | 1 |

the *SARIMA* model is determined using the Akaike information criterion (AIC). The *BPNN* has one hidden layer with 14 neurons. Additionally, *LSSVM* adopts a linear kernel function and obtains the corresponding values through parameter optimization. The *LSTM* model has 8 neurons in its first layer and 4 neurons in its second layer. By employing the *OLS* method, we obtain the parameters for three other models, including *SGM*, *SDTGM*, and *FTGM*.

Fig. 3 shows that the trend in America's oil consumption follows an initial decline followed by an increase with fluctuations over time. Several models, including *DGSTPM(1,1), SARIMA, SDTGM, LSSVM,* and *LSTM*, effectively capture this decreasing-then-increasing pattern in the oil consumption series. However, *SGM(1,1)* and *FTGM* models do not reflect this trend; their simulation and prediction curves consistently show an upward trajectory. Intuitively, both in terms of simulation and prediction stages, the new model's curve aligns more closely with the original sequence compared to the remaining eight models. The simulation curves of *SARIMA, LSSVM,* and *LSTM* models also demonstrate good agreement with the original values. Conversely, among all nine models considered, *BPNN* exhibits significant deviation from the original values in both simulation and prediction phases, suggesting its inadequacy for modeling the American oil consumption series.

Table 4 shows that the new model achieves the lowest errors in both simulation and prediction stages, with *MAPES, MAPEP, RMSES,* and *RMSEP* of 1.19 %, 0.67 %, 289.5, and 180.7, respectively, ranking first in terms of minimum *MAPE* and *RMSE* among all models. This phenomenon signifies that the new model outperforms others in accurately simulating and predicting American petroleum consumption data. Additionally, among the APE values for 12 predicted data points within nine forecasting models, those APE values generated by using the *DGSTPM(1,1)* model are all less than 2 %, with its minimum APE value at 0.06 %, displaying the smallest varied range. This result indicates that the proposed model outperforms other competitors at forecasting performance, making it a promising choice for reliable predictions in oil consumption. In the simulation phase, the new model has lower *MAPES* and *RMSES* than other competitors, confirming its superior simulation performance.

Moreover, the simulation accuracy *MAPES* and prediction accuracy *MAPEP* of six models, namely *DGSTPM(1,1), SGM(1,1), DGSTM(1,1), FTGM, SARIMA,* and *LSSVM*, are all lower than 2 %. This phenomenon indicates that these models are well-suited for capturing the patterns and trends presented in the American oil consumption sequences. It is noted that *BPNN* performed the least satisfactorily in both the simulation and prediction phases. The *BPNN* model yields the highest *MAPEP*, likely attributed to its unstable memory of network learning. This situation suggests that *BPNN* may struggle to effectively learn and replicate the patterns in the American petroleum consumption data, leading to less accurate simulations and predictions than the other models considered. Overall, the new model *DGSTPM(1,1)* with the cultural algorithm has better prediction ability than other competing models. It has the most ability to capture future trends and has an advantage in predicting large sample cases.

#### 3.4.2. Case two: Quarterly coke production in China

To further test the validity of the new model, this paper also selects quarterly coke production in China to compare with various prediction models. China holds the distinction of being the world's largest producer and consumer of coke, with coke playing a significant role in the country's energy landscape (Liu & Zhou, 2023). Accurate forecasting of coke production can offer valuable support for China's energy structure planning and adjustments. A total of thirty-two data points are collected from 2013 to 2020 to evaluate the effectiveness of the new model. Among them, twenty-eight observations from 2013Q1 to 2019Q4 are used as the in-sample set for training the model, while the remaining data points from 2020Q1 to 2020Q4 served as the out-of-sample set for measuring its forecasting performance. In this study, *DGSTPM(1,1)* and eight other competitive models are selected to forecast quarterly coke output in China and assess the modeling effect of the new approach under a small sample size. Table 5 presents their parameter estimations. Furthermore, as illustrated in Fig. 4, the coke yield series exhibits notable seasonal and periodic fluctuations despite the limited sample size.

In Fig. 4, during the simulation stage, the new *DGSTPM(1,1)* model stands out for its superior fitting with actual observations, effectively addressing the nonlinear trends and cyclical fluctuations inherent in the coke yield production sequence. This phenomenon may be attributed to the incorporation of the Cultural Algorithm, which enables the new model to accurately determine the time power index. While models such as *DGSTM(1,1), SGM(1,1), STDGM, SARIMA,* and *LSTM* are able to capture trend changes in the sequences during simulation stage, they are susceptible to extreme points and fail to adequately capture stochastic volatility of the series. On the other hand, the *BPNN* model requires a large amount of data for accurate simulation of the original sequence. Consequently, when dealing with small sample sizes (as in case two), its simulated coke yield production sequence deviates significantly from the original curve. Furthermore, during the prediction stage, it is apparent that the new *DGSTPM(1,1)* model captures the evolving trend of coke production, displaying forecasting curves that closely align with the actual values, outperforming the other models. While *DGSTM(1,1), SGM(1,1), SDTGM, FTGM, SARIMA*, and *LSTM* can broadly depict the curve's evolution, there are still inevitable error gaps compared to the actual values. Notably, *BPNN* and *LSSVM* deviate significantly from the original sequence change trend.

The forecasted results and error indices of the nine prediction models are presented in Table 6. When arranging the values in ascending order, the new model stands out by ranking first in all four indices: *MAPES, MAPEP, RMSES*, and *RMSEP*. These results unequivocally demonstrate the superior forecasting capability of the new model compared to the other eight models. Additionally, the *APE* values of the new model during the prediction phase consistently remain below 5 %, indicating high forecasting stability. In contrast, *BPNN* exhibits the poorest forecasting performance among the nine models, with a significantly higher *APE* value than the others and notable fluctuations within the range of all *APE* values. This intelligent model displays high instability when predicting time series with small sample sizes. Although *DGSTM(1,1), SGM(1,1), SDTGM, FTGM, SARIMA, LSSVM,* and *LSTM* perform better than *BPNN* in terms of prediction accuracy, there is still a noticeable gap compared to the new model's performance. Therefore, it can be concluded that the new model successfully predicts seasonal time sequences using large samples in case one while also being suitable for generating forecasts with limited sample sizes. Overall, this versatile approach effectively addresses both scenarios by showcasing high efficiency.

### 3.5. Comparisons of nine prediction models over the DM and SPA tests

The comparative analysis of the new model and its eight competing models, presented in Table 4 and Table 6, focuses on the magnitude of errors. However, it does not provide statistical substantiation for the effectiveness of the new model and highlight significant differences among the various models. This section employs two statistical tests, namely the Superior Predictive Ability (*SPA*) and the Diebold-Mariano (*DM*) tests, to assess the superiority of the new model and the differences in modeling the two cases among different models, thereby enhancing the robustness of the predictive results obtained using the new model. Table 7 presents the *DM* test results for two cases, using the new *DGSTPM(1,1)* model as the benchmark model. In Case one, which pertains to monthly crude oil consumption, the p-values for the error metric *APE* are all less than 0.1 for the eight comparison models, indicating significant differences between the modeling results of the new model and the other models. Additionally, all *DW* values are less than 0, implying higher modeling accuracy for the new model. In Case two, for both the APE metric and the SE measure, the p-values for the five models

(*DGSTM*, *SGM, SDTGM*, *BPNN*, and *LSTM*) are all less than 0.1, except for the *FTGM*, *SARIMA*, and *LSSVM* models, indicating significant differences between the new model and these five models as well.

Table 8 presents the SPA tests for the nine models across two cases. It can be observed that when the new *DGSTPM(1,1)* model serves as the benchmark model, the p-values for the SAP tests of the eight comparative models are all one under the error criteria APE and SE for both Case one and Case two. Conversely, when each of the eight comparative models serves as the benchmark model, the p-values for the *DGSTPM (1,1)* model are all 0. This phenomenon indicates that the predictive accuracy of the new model is statistically significantly higher than that of the eight comparative models for both cases, demonstrating its superiority over the others. Among the remaining models, some perform well in Case one, such as *SGM(1,1), DGSTM(1,1)*, and *FTGM*, while others perform better in Case two, such as *SARIMA* and *LSTM* models. *BPNN* exhibits the poorest predictive performance in both cases.

### 3.6. Summary of two cases

According to the empirical analysis of two cases, the following summary can be obtained:

(1) The new *DGSTPM(1,1)* model can deal with seasonal fluctuations under different sample size conditions effectively and keenly capture the trend characteristics of the original time sequence. From the simulative and predictive performance perspectives, the proposed model significantly outperforms the other eight seasonal models, including *DGSTM(1,1), SARIMA, BPNN, SDTGM, FTGM, SGM, LSSVM,* and *LSTM*. One of the reasons might be that the new model incorporates time power, which can effectively deal with the seasonality, periodicity, nonlinearity, and other characteristics of the seasonal sequences. Meanwhile, it helps to capture the trend signal of the seasonal series more sensitively. From the results of the *SPA* and *DM* tests, the *DGSTPM(1,1)* model outperforms the other comparison models in both cases, further suggesting the stability and robustness of the new model.
(2) As grey seasonal prediction models, *DGSTM(1,1)* and *FTGM(1,1)* have advantages in processing the seasonality of time series. The *SARIMA, LSSVM*, and *LSTM* models have achieved good fitting or forecasting accuracy for the two cases. However, none of these three models can achieve optimal performance simultaneously in both prediction and simulation stages. Furthermore, *BPNN*'s ability to simulate and predict the actual value is slightly inadequate due to insufficient data and excessive control parameters.
(3) Accurate predictions of the total petroleum consumption can provide support for planning in the oil industry, such as ensuring the production and purchase of the required amount of oil, thereby saving various time, manpower, and resource costs. Similarly, precise forecasts of coke production can assist in planning and refining coke production, leading to cost savings across various aspects.

## 4. Conclusion

The integration of a time power item into the *DGSTM(1,1)* framework spawns a novel model *DGSTPM(1,1)*, designed to enhance the predictive accuracy of seasonal sequences. Through meticulous case studies involving total oil consumption in the United States and coke production in China, key insights emerge: *DGSTPM(1,1)* is adept at handling seasonal time series with diverse sample sizes, showcasing nonlinear trends and periodic fluctuations. Leveraging the cultural algorithm bolsters the model's adaptability, enabling better resolution of the inherent nonlinearities in seasonal data and significantly amplifying its inclusiveness. Compared to grey (or grey hybrid) models, statistical econometric techniques, and machine learning methodologies, *DGSTPM (1,1)* demonstrates superior stability and robustness in forecasting performance. Moreover, a comprehensive exploration of the model's properties through mathematical analyses sheds light on its internal mechanisms, fostering a deeper comprehension.

Furthermore, the versatility of this newly established model paves the way for its deployment across various domains, such as the Fresh cold chain, emergency management, and natural disaster systems. However, the grey seasonal model proposed in this paper belongs to the grey system methodology, which is particularly effective for modeling systems with limited samples and sparse information. It may not be suitable for scenarios with abundant information and large sample sizes, where the utilization of the new model may result in significant errors. To tackle this challenge, traditional accumulation methods can be replaced with dynamic local accumulation in the *DGSTPM(1,1)* model. Moreover, the new model developed in this study exhibits a complex structure with numerous parameters, potentially leading to overfitting or substantial errors when applied to systems with limited data. In such instances, employing L1 or L2 regularization algorithms can help alleviate these concerns.

## CRediT authorship contribution statement

**Weijie Zhou:** Conceptualization, Software, Methodology, Funding acquisition, Validation, Writing – original draft, Writing – review & editing. **Jiaxin Chang:** Data curation, Validation, Writing – original draft, Writing – review & editing. **Huimin Jiang:** Data curation, Methodology, Validation, Writing – original draft. **Song Ding:** Data curation, Software, Methodology, Funding acquisition, Writing – original draft, Writing – review & editing. **Rongrong Jiang:** Data curation, Writing – original draft. **Xupeng Guo:** Data curation, Writing – original draft, Writing – review & editing, Validation.

## Declaration of competing interest

The authors declare that they have no known competing financial interests or personal relationships that could have appeared to influence the work reported in this paper.

## Data availability

Data will be made available on request.

## Acknowledgments

The authors appreciate the time of the editors and the anonymous reviewers for reviewing our paper. This work was funded by the National Natural Science Foundation of China (71701024, 71901191). Humanities and Social Science Fund of Ministry of Education of China (23YJC790016); Zhejiang Provincial Natural Science Foundation of China (LY24G010003); National Statistical Scientific Research Project (2023LY015); Zhejiang Educational Science Planning Project (2023SCG240). The National Social Science Fund, China (20CRK018, 21BJY007, 20BJL119); the Research and Innovation Program for Graduate Students in Jiangsu Province, China (KYCX20_2615); Graduate Research and Practice Innovation Program Project in Jiangsu (KYCX23_3008).

## References

ArunKumar, K. E., Kalaga, D. V., & Kumar, C. M. S. (2021). Forecasting the dynamics of cumulative COVID-19 cases (confirmed, recovered and deaths) for top-16 countries using statistical machine learning models: Auto-Regressive Integrated Moving Average (*ARIMA*) and Seasonal Auto-Regressive Integrated Moving Average (*SARIMA*). *Applied Soft Computing, 103*, Article 107161.

Carmona-Benítez, R. B., & Nieto, M. R. (2020). *SARIMA* damp trend grey forecasting model for airline industry. *Journal of Air Transport Management, 82*, Article 101736.

Chen, C. C., Chang, C. J., & Zhuang, Z. Y. (2020). An envelopment learning procedure for improving prediction accuracies of grey models. *Computers & Industrial Engineering, 139*, Article 106185.

Chen, C. I., & Huang, S. J. (2013). The necessary and sufficient condition for *GM (1, 1)* grey prediction model. *Applied Mathematics and Computation, 219*(11), 6152–6162.
Chen, H. B., Pei, L. L., & Zhao, Y. F. (2021). Forecasting seasonal variations in electricity consumption and electricity usage efficiency of industrial sectors using a grey modeling approach. *Energy, 222*, Article 119952.
Chen, Y. H., Yang, Y., & Liu, C. Q. (2015). A hybrid application algorithm based on the support vector machine and artificial intelligence: An example of electric load forecasting. *Applied Mathematical Modelling, 39*(9), 2617–2632.
Ding, S. (2019). A novel discrete grey multivariable model and its application in forecasting the output value of China's high-tech industries. *Computers & Industrial Engineering, 127*, 749–760.
Ding, S., Li, R. J., & Wu, S. (2021). Application of a novel structure-adaptative grey model with adjustable time power item for nuclear energy consumption forecasting. *Applied Energy, 298*, Article 117114.
Ding, S., & Zhang, H. H. (2023). Forecasting Chinese provincial $CO_2$ emissions: A universal and robust new-information-based grey model. *Energy Economics, 121*, Article 106685.
Ding, S., Hu, J. Q., & Lin, Q. Q. (2023). Accurate forecasts and comparative analysis of Chinese $CO_2$ emissions using a superior time-delay grey model. *Energy Economics, 126*, Article 107013.
Fang, T. T., & Lahdelma, R. (2016). Evaluation of a multiple linear regression model and *SARIMA* model in forecasting heat demand for district heating system. *Applied Energy, 179*, 544–552.
Farajzadeh, J., & Alizadeh, F. (2018). A hybrid linear–nonlinear approach to predict the monthly rainfall over the Urmia Lake watershed using wavelet-*SARIMAX-LSSVM* conjugated model. *Journal of Hydroinformatics, 20*(1), 246–262.
Gupta, P., & Christopher, S. A. (2009). Particulate matter air quality assessment using integrated surface, satellite, and meteorological products: Multiple regression approach. *Journal of Geophysical Research: Atmospheres, 114*, D14205.
Hu, J. B., & Chen, H. (2023). Will green fiscal policy influence the effect of green finance? From the perspective of reducing pollution and carbon emissions. *Collected Essays on Finance and Economics, 10*, 25–35.
Kaytez, F. (2020). A hybrid approach based on autoregressive integrated moving average and least-square support vector machine for long-term forecasting of net electricity consumption. *Energy, 197*, Article 117200.
Khwaja, A. S., Anpalagan, A., & Naeem, M. (2020). Joint bagged-boosted artificial neural networks: Using ensemble machine learning to improve short-term electricity load forecasting. *Electric Power Systems Research, 179*, Article 106080.
Li, D. Y., Liu, L. Y., & Lv, H. T. (2021). Prediction of China's housing price based on a novel grey seasonal model. *Mathematical Problems in Engineering, 2021*, 1–11.
Li, K. Q., Liang, C. Y., & Lu, W. X. (2020). Forecasting of short-term daily tourist flow based on seasonal clustering method and *PSO-LSSVM*. *ISPRS International Journal of Geo-Information, 9*(11), 676.
Li, N., Wang, J. L., & Wu, L. F. (2021). Predicting monthly natural gas production in China using a novel grey seasonal model with particle swarm optimization. *Energy, 215*, Article 119118.
Li, X. M., Li, N., Ding, S., Cao, Y., & Li, Y. (2023). A novel data-driven seasonal multivariable grey model for seasonal time series forecasting. *Information Sciences, 642*, Article 119165.
Liu, C., Xie, W. L., & Lao, T. F. (2020). Application of a novel grey forecasting model with time power term to predict China's GDP. *Grey Systems: Theory and Application, 11*, 343–357.
Liu, X. Y., Peng, H. Q., & Bai, Y. (2014). Tourism flows prediction based on an improved grey *GM (1, 1)* model. *Procedia-Social and Behavioral Sciences, 138*, 767–775.
Liu, Y. W., & Zhou, S. C. (2023). The coordination mechanism of formal and informal environmental regulation reducing pollution and carbon emission benefits. *Collected Essays on Finance and Economics, 8*, 103–112.
Lu, S. Q., Zhang, Q. Y., & Chen, G. S. (2021). A combined method for short-term traffic flow prediction based on recurrent neural network. *Alexandria Engineering Journal, 60*(1), 87–94.
Mao, Q., Zhang, K., & Yan, W. (2018). Forecasting the incidence of tuberculosis in China using the seasonal auto-regressive integrated moving average (*SARIMA*) model. *Journal of Infection and Public Health, 11*(5), 707–712.
Martínez, F., Frías, M. P., & Pérez-Godoy, M. D. (2018). Dealing with seasonality by narrowing the training set in time series forecasting with kNN. *Expert Systems with Applications, 103*, 38–48.
Mwanga, D., Ong'ala, J., & Orwa, G. (2017). Modeling sugarcane yields in the Kenya sugar industry: A *SARIMA* model forecasting approach. *International Journal of Statistics and Applications, 7*(6), 280–288.
Nourani, V., & Behfar, N. (2021). Multi-station runoff-sediment modeling using seasonal *LSTM* models. *Journal of Hydrology, 1*, Article 126672.
Qian, W. Y., Dang, Y. G., & Liu, S. F. (2012). Grey *GM (1,1, ta)* model with time power term and its application. *System Engineering Theory and Practice, 32*, 2247–2252.
Reynolds, R. G. (1994). An introduction to cultural algorithms[C]//Proceedings of the third annual conference on evolutionary programming. *River Edge: World Scientific*, *24*, 131-139.
Saz, G. (2011). The efficacy of SARIMA models for forecasting inflation rates in developing countries: The case for Turkey. *International Research Journal of Finance and Economics, 62*, 111–142.
Tang, L., Yu, L. A., & He, K. (2014). A novel data-characteristic-driven modeling methodology for nuclear energy consumption forecasting. *Applied Energy, 128*, 1–14.
Tsui, W. H. K., Balli, H. O., & Gilbey, A. (2014). Forecasting of Hong Kong airport's passenger throughput. *Tourism Management, 42*, 62–76.
Valipour, M. (2015). Long-term runoff study using *SARIMA* and *ARIMA* models in the United States. *Meteorological Applications, 22*(3), 592–598.
Wang, X. W., Cai, Y. P., & Xu, Y. (2014). Optimal strategies for carbon reduction at dual levels in China based on a hybrid nonlinear grey-prediction and quota-allocation model. *Journal of Cleaner Production, 83*, 185–193.
Wang, Z. X., Li, Q., & Pei, L. L. (2018). A seasonal *GM (1, 1)* model for forecasting the electricity consumption of the primary economic sectors. *Energy*, *154*, 522-534. https://doi.org/10.1016/j.energy.2018.04.155.
Wang, Z. X., Wang, Z. W., & Li, Q. (2020). Forecasting the industrial solar energy consumption using a novel seasonal GM (1, 1) model with dynamic seasonal adjustment factors. *Energy, 200*, Article 117460.
Wei, B. L., Xie, N. M., & Yang, L. (2020). Understanding cumulative sum operator in grey prediction model with integral matching. *Communications in Nonlinear Science and Numerical Simulation, 82*, Article 105076.
Xiao, X. P., & Duan, H. M. (2020). A new grey model for traffic flow mechanics. *Engineering Applications of Artificial Intelligence, 88*, Article 103350.
Xiao, X. P., Yang, J. W., & Mao, S. H. (2017). An improved seasonal rolling grey forecasting model using a cycle truncation accumulated generating operation for traffic flow. *Applied Mathematical Modelling, 51*, 386–404.
Xiong, X., Hu, X., & Guo, H. (2021). A hybrid optimized grey seasonal variation index model improved by whale optimization algorithm for forecasting the residential electricity consumption. *Energy, 4*, Article 121127.
Ye, L. L., Xie, N. M., John, E. B., & Shang, Z. J. (2024). Forecasting seasonal demand for retail: A Fourier time-varying grey model. *International Journal of Forecasting, 18*. https://doi.org/10.1016/j.ijforecast.2023.12.006
Yuan, C., Liu, S., & Fang, Z. (2016). Comparison of China's primary energy consumption forecasting by using ARIMA (the autoregressive integrated moving average) model and *GM (1, 1)* model. *Energy, 100*, 384–390.
Zhou, W. J., & Ding, S. (2021). A novel discrete grey seasonal model and its applications. *Communications in Nonlinear Science and Numerical Simulation, 93*, Article 105493.
Zhou, W. J., Jiang, R. R., Ding, S., Cheng, Y. K., Li, Y., & Tao, H. H. (2021). A novel grey prediction model for seasonal time series. *Knowledge-Based Systems, 229*, Article 107363.
Zhou, W. J., Tao, H. H., Chang, J. X., Jiang, H. M., & Chen, L. (2023). Forecasting Chinese electricity consumption based on grey seasonal model with new information priority. *Sustainability, 15*, 3521. https://doi.org/10.3390/su15043521
Zhou, W. J., Wu, X. L., & Ding, S. (2020). Predictive analysis of the air quality indicators in the Yangtze River Delta in China: An application of a novel seasonal grey model. *Science of The Total Environment, 748*, Article 141428.
Zhou, W., & He, J. M. (2013). Generalized GM (1, 1) model and its application in forecasting of fuel production. *Applied Mathematical Modelling, 37*(9), 6234–6243.
Zou, J. G., Bui, K. T., & Xiao, Y. X. (2018). Dam deformation analysis based on *BPNN* merging models. *Geo-Spatial Information Science, 21*(2), 149–157.